Percolation Theory-Analysis of Malware Epidemics in Large-Scale Wireless Networks

Thesis by

Ainur Zhaikhan

In Partial Fulfillment of the Requirements

For the Degree of

Master of Science

King Abdullah University of Science and Technology, Thuwal,

Kingdom of Saudi Arabia

EXAMINATION COMMITTEE PAGE

The thesis of Ainur Zhaikhan is approved by the examination committee:

Committee Chairperson: Mohamed-Slim Alouini

Committee Member: Basem Shihada, Osama Amin

ABSTRACT

Percolation Theory for Analysis of Large Scale Network Epidemics

Ainur Zhaikhan

The foreseen massive deployment of the internet of things (IoT) is expected to suffer from high security risks. This mainly results from the difficulty to monitor and cure the IoT devices in such large-scale deployment. In this thesis, we propose a spatial random deployment of special nodes (firewalls) which can detect and cure infected nodes within certain radius. An important concern is to add sufficient number of firewalls to make an epidemics finite and, hence, prevent malware outbreak over the whole network. The problem will be analyzed using percolation theory. Namely, we derive an upperbound for the critical intensity of spatial firewalls which guarantees prevention of large-scale network epidemics, regardless of the intensity of regular nodes. Using tools from percolation theory, we analyze the proposed solution and show the conditions required to ensure its efficiency.

ACKNOWLEDGEMENTS

I would like to express my gratitude to my supervisor, Professor Mohamed-Slim Alouini, for his continious support, encouragement, and guidance.

I would like also to thank Doctor Mustafa Kishk for his patience, valuable help, guidance and critical evaluation throughout the course of this work. His expertise in stochastic geometry and percolation theory helped me to solve many complex problems that I faced during this thesis.

I would like also to thank Professor Hesham Elsawy from King Fahd University of petroleum and minerals for his precious help and useful advice during all the steps of this work.

I am also thankful to all my friends at KAUST for making this experience at this lovely university very enjoyable and exciting.

Finally, I am deeply grateful to my beloved parents, my sister, my brother, my sweet nieces and nephews for their unconditional love and support.

TABLE OF CONTENTS

LIST OF ABBREVIATIONS

RGG	Random Geometric Graph
ARG	Abstract Random Graph
CRN	Cognitive Radio Network
PN	Primary Network
SN	Secondary Network
SG	Secrecy Graph
PPP	Poisson Point Process
PDF	Probability Density Function
CDF	Cumulative Distribution Function

LIST OF SYMBOLS

V	Set of Vertices
E	Set of Edges
$G(\cdot)$	Graph
$\mathcal{L}_{\square}$	Lattice
$\mathcal{L}'_{\square}$	Dual Lattice
$\theta(\cdot)$	Percolation probability
$\mathcal{K}^{\square}(0)$	Connected component including the origin

LIST OF FIGURES

Chapter 1

Introduction

1.1 Context and Motivation

Due to continuous increase in the number of IoT devices, networks are becoming more vulnerable to illegitimate intrusions and malware spread. Hence, a secure connection over long distances is a current major concern. To make the vulnerability problem clear, consider a wireless communication network where, at a certain instance, a malware originates at one of the communication devices and spreads in an epidemic manner from each node to its neighbors. To prevent such malware outbreak, we propose to deploy nodes with high capabilities (spatial firewalls) that can cure all devices falling within their detection ranges. An obvious important concern here is the minimum intensity of firewalls that will assure blockage of epidemics. We use tools from *percolation theory* to analyze considered setup and optimize the proposed solution.

1.2 Thesis Organization

To understand percolation theory we will need a notion of random graphs. So, in Chapter 2 along with introduction of percolation theory we will define random graphs and explain their classifications. Next, in Chapter 3 will make a detailed survey on the use of percolation theory in wireless communication network. Finally, in Chapter 4 our work will narrow down on the application of percolation theory for the network epidemics problem. At the same chapter the analysis of the proposed solution will be

supported with simulation results.

Chapter 2

Percolation Theory and Random Graphs

2.1 Introduction

In this chapter, we provide background on Percolation Theory and Random Graphs.

2.2 Percolation Theory

2.2.1 Percolation Basics

Percolation theory was introduced in 1957 by Broadment and Hammersley to model liquid penetration through porous material [1]. Later, it was used to address more substantial topics such as fire spread across forests, epidemics in orchards, water filtration through rocks, disease spread, the effective resistance of mixed conductors [2] as well as network connectivity.

To understand the nature of percolation phenomenon let us study the following basic model. Consider underlying a 2-dimensional square lattice $\mathcal{L}^s := G(V, E)$ framed with vertex set $V = \mathbb{Z}^2$ and edge set $E = \{(x, y) \in V^2 : ||x - y|| = 1\}$. With the condition that each edge in $\mathcal{L}^s$ exists independently with probability p, G(V,E) turns to *random graph*. The tuning parameter p can be used to control the connectivity of $\mathcal{L}^s$. In particular, a sufficiently small value of p may give several connected components (See Definition 1). As we increase p, these connected components merge to constitute larger components and at some value of p we may observe an infinite connected component, also called a *giant component* [2]. The phenomenon of existence of giant component and its probability is called *percolation* and *percolation*

probability, respectively.

Definition 1 (Connected Component)**.** A connected component is a sub-graph $K \subseteq G(V, E)$ with the largest possible elements such that within K any vertex $x_i \in K$ can always find a root through a set of consecutive edges to any other vertex $x_j \in K$, $i \neq j$.

Note: It is a common practice to specify a connected component with its single element. So, for example, $K(O)$ denotes a connected component containing the origin.

Definition 2 (Percolation Probability)**.** Percolation probability is the probability of existence of infinitely large connected component, i.e

$$\theta(p) = Pr(|K(O)))| = \infty). \tag{2.1}$$

Formally, percolation is characterized with the following behavior

$$\begin{aligned} \theta(p) &> 0, \quad \text{for } p < p_c \\ \theta(p) &= 0, \quad \text{for } p > p_c. \end{aligned} \tag{2.2}$$

In addition, we can say that $\theta(p)$ is a non-decreasing function of p and transition from non-connectivity to connectivity state happens rather rapid (Kolmogorov Zero-One law). So, A phenomenon occurring at p_c is named *a phase transition*.

In the aforementioned case, when p is the probability associated with edges, we say a *bond percolation* is happening in $\mathcal{L}^s$. If the same condition is applied to vertices, instead of edges, then it turns to a *site percolation*. Removal of a particular site removes all edges associated with it. Hence, upon a proper transformation, a bond percolation can be viewed as a special case of site percolation [3].

Another important characteristic of a percolating network is the mean out/in - degree of the node, defined below. The difference between in and out-degree comes from possible directivity of edges.

Definition 3 (Out/In Degree [4])**.** In-degree of node n is the number of direct links from other nodes (transmitters) to the node n (a receiver). Out-degree of node n is the number of direct links from node n (transmitter) to the other nodes in the network (receivers).

2.2.2 Useful properties of some percolation models

Now, we will list useful identities and inequalities related to critical probabilities in bond (p_c^b) and site (p_c^s) percolation models

1. For any infinite graph G, $p_c^s(G)$ is lowerbounded with $p_c^b(G)$.

2. For any 2D lattice $\mathcal{L}$ and its dual $\mathcal{L}'$ (see Definition 4) the following is hold

$$p_c^b(\mathcal{L}) + p_c^b(\mathcal{L}') = 1.$$

3. Let $\mathcal{L}^d$ be 2D lattice recast from $\mathcal{L}$ by creating edges along all diagonals of all faces in $\mathcal{L}$. Then for any planar $\mathcal{L}$ and $\mathcal{L}^d$,

$$p_c^s(\mathcal{L}) + p_c^s(\mathcal{L}^d) = 1.$$

.

4. Let p^h and p^v denote probabilities of horizontal and vertical link in square lattice. Then in bond percolation model corresponding critical probabilities satisfy (Sykes-Essam theory [5])

$$p_c^h + p_c^v = 1.$$

.

Table 2.1: Critical probability for popular planar lattice models

Lattice type	**Percolation model**	$\mathbf{p_c}$
Square	bond	$\frac{1}{2}$ (Harris-Kesten theorem)
Triangular	bond	$2\sin(\frac{\pi}{18})$
	site	$\frac{1}{2}$
Hexagonal (Honeycomb)	bond	$1-2\sin(\frac{\pi}{18})$
	site	0.593
	face[1]	$\frac{1}{2}$

5. Let a triangular lattice have a site retention probability p^s and bond probabilities p^{b_1}, p^{b_2} and p^{b_3}, then corresponding critical probabilities follow [6]

$$p_c^s\left(p_c^{b_1}+p_c^{b_2}+p_c^{b_3}-p_c^{b_1}p_c^{b_2}p_c^{b_3}\right)=1.$$

In general, percolation over regular structures such as lattices are well understood and studied in the literature. So, continuum percolation problems such as in random geometric graphs are usually solved by mapping continuum percolation to discrete one. Therefore, in Table 2.1, we provide known percolation thresholds for some lattice models.

Definition 4 (Dual Lattice)**.** Dual of the lattice is obtained by drawing bisectors to each bond of an original lattice and taking intersection points of those bisectors as vertices of a new lattice. Hence, dual of the square, triangular, and hexagonal lattices are square, hexagonal, and triangular lattices, respectively.

2.3 Classification of Random Graphs

2.3.1 Introduction to Random Graphs

All graphs associated with some source of randomness, e.g., random edges/sites or randomness due to the spatial location of nodes, form a big class of random graphs.

[1] equivalent to site percolation in triangular lattice

Figure 2.1: Random Graph Taxonomy

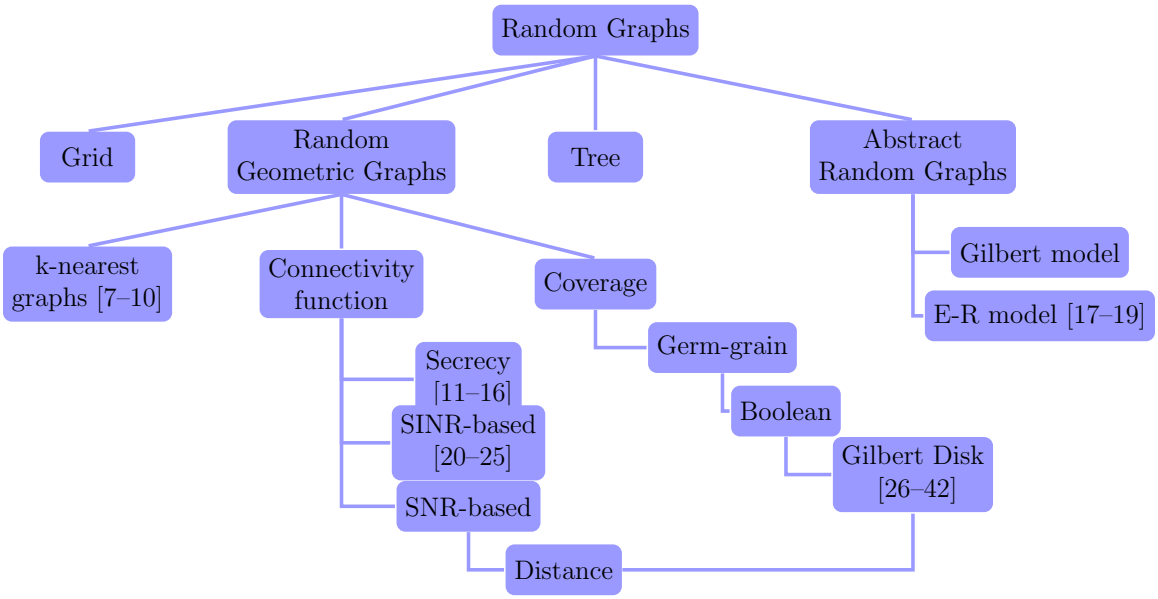

Popular types of random graphs are grids (latices), trees, random geometric, and abstract random graphs (RGGs and ARGs), as shown in Fig.2.1. The first two are structured graphs. *Grids* have a certain underlying geometric structure which becomes random due to uncertainty in a site or/and bond retention. *Trees* have a hierarchical structure where the number of node offsprings is random.

Definition 5 (Random Geometric Graph)**.** Random geometric graph is a graph type where vertices are randomly scattered on $\mathcal{R}^d$, and the existence of edges depends on the location of vertices.

Due to fewer restrictions in the structure, RGGs have more practical sense, and they are mainly used to model physical networks (e.g., a wireless communication network). However, structured graphs are easier to study and, hence, for them, there are more known percolation thresholds, as discussed in Sec. 2.2.2. So, commonly percolation study in RGGs comes coupled with analysis of a lattice or tree models.

Definition 6 (Abstract Random Graphs)**.** Abstract randoms graphs are graph types where the location of vertices is of no importance, and edges are created randomly

regardless of the spatial distribution of vertices.

Due to the abstractness of vertex locations, this type of graphs is used to model virtual networks such as computer networks. Subcategories of RGGs and ARGs are described in the following sections.

2.3.2 Random Geometric Graphs

As the existence of links is dependent on the spatial distribution of nodes, a wireless communication network is mainly modeled with random geometric graphs (RGGs) [7–16, 20–27, 29–34, 43–62]. A connection between nodes can be defined with a connectivity function, e.g., based on distance, SNR, Signal-to-Interference-Ratio (SINR), Secrecy rate. Another approach is coverage models [26–31], where each node is associated with some predefined coverage region that frame potential locations for connectable nodes.

Connectivity based RGGs

SNR-based RGGs can be viewed as a special case of SINR RGGs, while distance-based RGG is equivalent to Gilbert Disk coverage model, discussed in Sec.2.3.2. So, to avoid repetitions, we will only define only SINR- and secrecy- based RGGs.

Signal-to-Interference-Ratio Graphs (STIRG) STIRG was first introduced by Douse et al. [63, 64]. It is a model where single hop connection between two nodes depends not only on the spatial separation between them , but the interference level caused by other nodes in the network. So formally, connectivity function for SITRG is

$$\overrightarrow{E} = \left\{ \overrightarrow{x_i x_j} : \frac{P_i l\left(x_i - x_j\right)}{N_0 + \gamma \sum_{k \neq i,j} P_k l\left(x_k - x_j\right)} \geq \beta \right\}, \tag{2.3}$$

where P_i is a transmit power of the node i, $l\left(x_i - x_j\right)$ is a path loss between nodes i and j, N_0 is noise power, β is SINR threshold, and $0 \leq \gamma \leq 1$ are inverse of processing

gain of the system which abstracts imperfections in orthogonality of coding scheme. Note overhead arrows in (2.3) which means that edges in the graph can be directional, unlike in distance based models. However, original model of STIRG introduced by Douse et al. [63] assumed bidirectional links, i.e. conditions of edge existence are satisfied both in $x_i \to x_j$ and $x_j \to x_i$ directions.

Secrecy Graphs Connectivity function for Secrecy graph is

$$\overrightarrow{E} = \{x_i x_j : \mathcal{R}_{\mathrm{s}}(x_i, x_j) > r_s\}, \tag{2.4}$$

where $\mathcal{R}_{\mathrm{s}}(x_i, x_j)$, called a maximum secrecy rate, is a rate measured relative to the highest eavesdropper rate in the network ($\mathcal{R}_{\mathrm{e}^*}$).

$$\mathcal{R}_{\mathrm{s}}(x_i, x_j) = [\mathcal{R}(x_o)]^+, \tag{2.5}$$

and r_s is a fixed threshold.

Unlike in distance/Gilbert disk case, there is no analogy of a secrecy graph among coverage models [65].

Coverage models

Gilbert Disk In Gilbert Disk graph $G(\lambda, r)$ points are spatially distributed according to Poisson Point Process (PPP) Φ with density λ and vertices $(x, y) \in \Phi$ create an edge iff they are within distance r from each other.

Germ-grain model Germ-grain can be viewed as a generalization of Gilbert Disk model. Germs (points) are scattered on R^d as a point process and coverage region(set of grains) is of arbitrary shape.

[2] $x^+ = max(x, 0)$

k-nearest graphs

It is an undirected graph type where two spatially scattered nodes are connected if either is at most k-th closest neighbor of the other one. A special case when $k = 1$ is called the nearest neighbor graph. One of the earliest works related to continuum percolation in k-nearest graphs is credited to Haggstrom and Meester (1996) [7].They proved that for $k = 1$ (the nearest neighbor) percolation is impossible in any dimension d (trivially except $d = 1$), while for $k = 2$ percolation may occur for some finite d. More recent work by Shang-Hua and Y.Frances [8] showed that for any finite dimension $d > 1$ there is always a threshold k_d which assures phase transition, in particular, for planar case (d=2) $k_2 < 213$. Later, Balister and Bollobas found a tighter bound $k_2 < 11$ [9]. Connectivity of k-nearest graph was also studied for finite area case. In finite k-nearest graph with area A under PPP assumption with intensity 1, a percolation probability tends to zero for $k < 0.074 \log A$, and tends to 1 for $k > 5.1774 \log A$, as $A \to \infty$ [10]. Ballister et al. [66] improved these results to $0.3043 \log A$ and $0.5139 \log A$ respectively

2.3.3 Abstract Random Graphs

Gilbert model

$G(n, p)$ is Gilbert random graph with n vertices and where any two distinct vertices create an edge independently from other edges with probability p. Hence,

$$P(G(n,p)\text{has M edges}) = p^M (1-p)^{\binom{n}{2}-M}. \tag{2.6}$$

Erdos-Renyi (ER)

In ER model a graph $G(n, M)$ with n vertices and M edges is chosen uniformly random from space of all possible graphs with n vertices and M edges. So, probability of a

single ER graph is

$$P(G) = \binom{\binom{n}{2}}{M}^{-1}. \tag{2.7}$$

2.4 Conclusion

In this chapter, we provided relevant information about the percolation theory and Random graphs so that a reader will feel comfortable with concepts, terms, and notations used further.

Chapter 3

Survey about Percolation Theory in Wireless Communication Network

3.1 Introduction

In this chapter, we will discuss in more detail the types of graphs that are popular for modeling of wireless communication networks and present related works. Percolation theory in wireless networks is mainly used to study connectivity and secrecy of the network. Therefore, the two main sections of the chapter will be dedicated to these two subjects.

3.2 Percolation and Connectivity

3.2.1 Gilbert disk model

Gilbert disk is popular in modeling wireless sensor networks (WSN). Connectivity of WSN based on Gilbert disk model was studied in [39]. One of the applications of WSN is to detect intrusion or motion of an object within the interested region. So, in this kind of application, it is not necessary to exploit the whole network area. Instead, coverage of interested exposure path is sufficient. With this in mind, in [35], Liu et al. applied site and bond percolation models, respectively, to find densities that prevent path exposure. Based on site percolation, authors in [38] derived the critical density of nodes to prevent exposure path in WSN with directional and omnidirectional sensors. The 3D scenario of exposure path problem was considered in [36], while general connectivity in 3D wireless sensor network was analyzed in [37]. In particular, authors

in [37] found critical density for coverage and connectivity in 3D WSN.

With regard to other applications, percolation in Gilbert disk model was also used to estimate node location in finite size network [40]. According to [40], the percolation threshold is computed to guarantee that message will reach the borders of the network, and the source site is predicted by measuring time delays. In addition, Gilbert Disk model was used to study connectivity in urban areas [41] and in the Swarm Robot network [42].

3.2.2 SNR graphs

In literature, SNR RGGs are usually simplified to basic distance-based RGGs. So, works dedicated to purely SNR percolation models are scarce. As a special case of the SINR graph, the directed SNR graph was studied in [67]. In particular, authors in [67] found the following bounds for λ_c

$$\lambda_c < \frac{4 \ln 2}{\left(\pi - 6 \sin^{-1}\left(\frac{1}{4}\right) - \frac{3\sqrt{3}(\sqrt{5}-1)}{8}\right) r_{\min}^2}, \tag{3.1}$$

$$\lambda_c \geq \frac{1}{[1 - C_t'] \, \pi \int_{r_{min}}^{r_{max}} g(r) f_R(r) dr}, \tag{3.2}$$

where

$$\begin{aligned} R &= L^{-1}\left(\frac{N_0 \beta}{P}\right), \\ r_{min} &= l^{-1}\left(\frac{N_0 \beta}{p_{\min}}\right), \\ r_{max} &= l^{-1}\left(\frac{N_0 \beta}{p_{\max}}\right), \end{aligned} \tag{3.3}$$

f_R and F_R is a probability density function (PDF) and cumulative distribution function (CDF) of R, respectively

$$g(r) = r^2 + 2 \int_r^{r_{max}} r' \left[1 - F_R\left(r'\right)\right] dr', \tag{3.4}$$

p_{min} is the minimum transmit power assuming that transmit power of nodes P can take values between $[p_{min}\ p_{max}]$ according to some distribution $f_P(p)$; C'_t is the t-th order cluster coefficient (for more details see [67]).

3.2.3 Interference-limited models

In SINR graphs, direct connectivity between two nodes does not only depend on their spatial location, but locations and powers of other nodes participating in the network. More formal definition can be found in Sec.2.3.2. One of the earliest works in SINR based percolation models is Dousse et al [63, 64]. They proved the following lemma.

Lemma 1 (Node degree in SITRG [63, 64])**.** *In SITRGs with finite support path loss function a node degree cannot exceed* $(1 + \frac{1}{\gamma\beta})$.

They reinforce finite support assumption for path loss function which means that for some $d < \infty$ $l(x) = 0$ when $x > d$. In addition $l(x)$ must be non-increasing and isotropic. Finiteness of path loss function is important for the simplicity of dealing with dependent edges. To have fair mapping, they define an open edge in square lattice such that percolation in square lattice assures continuum percolation in an original random graph. Namely, the definition of an open edge assures direct connectivity of any two nodes falling within two squares adjacent to the edge. Due to the interference-based definition of connectivity, not only adjacent squares need to be sufficiently occupied. Also, a total number of nodes within these two squares and their direct neighbors (sharing at least one common edge) must not exceed some threshold number (derived explicitly in [21]). As the definition of open edge covers more than just direct neighborhood (two adjacent squares to the edge), we may deal with the dependency of edges, unlike in the Boolean model. In other words, the probability of one edge is open will be correlated with the state of other neighboring edges. At this stage, if path loss was defined over an infinite domain, it would be difficult to frame the independence conditions of edges finitely. In practice, if nodes

were allowed to communicate over infinite distances, it would be difficult to have an idea about interference level at a node. So, some assumptions are required. In their system model, tuning parameters are γ and λ, which are inverse of system processing gain and density of nodes, respectively. By simulation they show percolation region in (λ, γ) space. Hence, they framed sub-critical and super-critical regions for the given model. In addition, they rigorously proved Lemma 2 given as follows.

Lemma 2 (Percolation in SITRG [63, 64])**.** *Let λ_c^0 be a critical density of nodes in SITRGs with finite support path loss function when $\gamma = 0$. Then for $\forall \lambda > \lambda_c^0$, $\exists\ \gamma^c$ such that $\forall \gamma < \gamma_c$ the given model percolates.*

In addition, they proved that no percolation occurs if $\gamma > 1/\beta$ or $\lambda < \lambda_c^0$. As it can be recalled from Sec.2.3.2 γ is a coefficient depending on the coding/decoding strategy of the system. Douse et al. [63,64] made an analysis for two coding schemes, CDMA and TDMA. In the CDMA scenario, all nodes get active at the same time, while in the latter case, the time interval is divided into n time slots, and each node activates every interval at i-th time slot randomly chosen from $1, 2...n$. Small values of γ inherent to CDMA schemes are usually complex to realize and have little practical sense. Using the well-known property of percolation that the time-slotted realization of the network improves connectivity, they proved that percolation condition could be better reached with TDMA as γ gets scaled with factor $1/n$.

Douse et al. omitted finite support assumptions in [68]. Instead, the following constraints were added

1. $l(x, y)$ is a function of absolute value of the distance between x and y (i.e $l(|x - y|)$)
2. $l(|x - y|)$ is strictly decreasing function, where $l(|x - y|) \leq 1$
3. $l(0) > \beta N/p$

4. $\int_0^\infty xl(x)\mathrm{d}x < \infty$

Even though unbounded support constraint was removed, condition 4 assures that interference at a node is finite [69].

The new definition of open edge for the given SINR model was based on the following two conditions

1. *Occupancy of the neighbourhood of the edge.* Let the neighbourhood be parametrized with some $d > 0$. Then occupancy implies left to right crossing of rectangle

$$[x_a - 3d/4, x_a + 3d/4] \times [y_a - d/4, y_a + d/4],$$

and top to bottom crossing of squares

$$[x_a - 3d/4, x_a - d/4] \times [y_a - d/4, y_a + d/4],$$

and

$$[x_a + d/4, x_a + 3d/4]\,[y_a - d/4, y_a + d/4],$$

where (x_a, y_a) are the middle point coordinates of the considered edge.

2. *Shifted shot noise limit.* Shifted shot noise at the receiver which is defined as follows

$$\tilde{I}(z) = \sum_k \tilde{l}\left(|z - x_k|\right),$$

where

$$\tilde{l}(x) = \begin{cases} l(0), & x \le \frac{\sqrt{10}d}{4} \\ l\left(x - \frac{\sqrt{10}d}{4}\right), & x > \frac{\sqrt{10}d}{4} \end{cases}$$

must not exceed some predefined threshold M.

With proper choice of M and N [68] proved validity of Theorem 1 and Theorem 3 also for unbounded support case.

Authors in [67] apply the same assumptions for path loss function as in [68]. Applying mapping to hexagonal lattice with side length d, they derived lower and upper bounds for critical $\gamma = \gamma_c$ in relation to λ

$$\vec{\gamma}_c(\lambda) \leq \frac{c_2}{\lambda - c_2'}, \tag{3.5}$$

where

$$\begin{aligned} c_2 &= \tfrac{2\sqrt{3}(p_{\max} - \beta N_0)}{9(1-\theta)\beta p_{\min} l(2d) d^2}, \\ c_2' &= \tfrac{2\sqrt{3}}{3(1-\theta)d^2}, \end{aligned} \tag{3.6}$$

$$\theta = \frac{\sqrt{10}}{d\sqrt[4]{27}\sqrt{\lambda_c}}. \tag{3.7}$$

R.Vaze in [70] fixed $\gamma = 1$ and proved that for large enough β, there is a closed interval of λ within which percolation probability is 0 and for small enough β there is the corresponding interval for strictly positive percolation probability. Then they make an analysis for a finite area network with n number of nodes. For the analysis, they use colored square lattice where each different colored squares depict nodes having orthogonal signals. Thus, only nodes corresponding to the same color square can interfere. They show that a sufficient number of colors that assures full connectivity of the network with high probability is $\mathcal{O}(\log n)$. For the case when transmit powers are no more fixed but i.i.d random variables authors in [71] derived an interesting result that $\gamma_c \leq 1/(2\beta)$ for $\forall\lambda$, $\beta > 0$.

Applications

Authors in [72] use percolation theory to study unicast capacity in the ad-hoc network with SINR assumption. [73] applies SINR percolation model to study multicast capacity of wireless ad-hoc networks under Gaussian channel model. SINR models in

Table 3.1: Notations

Term	Description	Term	Description
r_p r_s	Communication range of primary nodes Communication range of secondary nodes	P_d P_f	Probability of detection Probability of false alarm
R_I	Interference range of primary receivers	P_N	Noise power
r_I	Interference range of secondary receivers	P_{PT}	Transmit power
λ_p	Density of primary transmitters	σ	Path loss coefficient
λ_s	Density of secondary nodes	ϵ	Outage probability threshold
$\lambda_c(1)$	Critical intensity of nodes for Boolean model with unit communication range	N	Number of channels

more complex networks such as cognitive radio and secrecy graphs are discussed in details in the following sections.

3.2.4 Heterogeneous network (Cognitive Radio)

A typical cognitive radio model consists of primary and secondary networks. As the name implies, primary network (PN) is the first priority in spectrum access. Two secondary nodes intending to communicate in single-hop must satisfy both their own connectivity conditions and some tolerances of primary nodes varying from case to case.

The most common scenario of CRN is studied by W.Ren et al. in [56, 57], where secondary and primary nodes have some fixed communication ranges r_s and r_p, respectively and fixed interference tolerance distances for primary and secondary receivers R_I and r_I respectively. So, in order to have an edge between two secondary nodes, they should be at a distance less than r_s from each other and at least R_I and r_I far away from primary receivers and transmitters, respectively. The locations of primary and secondary nodes are modeled as two independent PPPs with densities λ_p and λ_s correspondingly. Each primary transmitter has one primary receiver placed uniformly at random within a circular region centered at the corresponding transmitter

and with radius R_p. Hence, PPP of primary receivers is dependent on PPP of primary transmitters, and both processes have the same density. The authors studied the effect of (λ_s, λ_p) pair on the connectivity of secondary networks (SNs) and defined connectivity region, which depicts all values of (λ_s, λ_p) resulting in percolation of secondary networks. Applying the Boolean continuum percolation model and the concept of the infinite vacant component, they found useful bounds and conditions for the connectivity region. First one is the condition for the intensity of primary transmitters that assures no percolation of secondary network regardless λ_s

$$\lambda_p \geq \frac{\lambda_{\mathrm{c}}(1)}{4\max\left\{R_I^2, r_I^2\right\} - r_s^2}. \tag{3.8}$$

Second one is a sufficient condition for connectivity given as

$$\lambda_p < \frac{1}{\pi\left[R_I^2 + r_I^2 - I\left(R_I, r_p, r_I\right)\right]} \ln \frac{1 - \exp\left(-\frac{\lambda_s r_s^2}{8}\right)}{1 - \left(\frac{1}{3}\right)^{(2k+1)^2}}, \tag{3.9}$$

where

$$k = \left\lceil 8\max\left\{R_I + \frac{r_s}{4}, r_I + \frac{r_s}{4}\right\}/r_s \right\rceil - 1, \tag{3.10}$$

$$I\left\{r, r_p, r_I\right\rangle = 2\int_0^r t\frac{S_I\left(t, r_p; r_I\right)}{\pi r_p^2}\mathrm{d}, \tag{3.11}$$

$S_I\left(t, R_p; r_I\right)$ is the area of intersection of two circles with centers at a distance of t and respective radii R_p and r_I.

[58] consider a similar scenario but with multiple channels. Connectivity between secondary nodes is a function of two parameters: communication range and probability of channel availability. Multiple channel condition can modelled as overlay of multiple PPP distributed primary networks of intensity λ_p. Hence, using the definition of PPP the probability of one channel availability for two secondary nodes can be written as

$$P = e^{-\lambda_p \gamma_1 \pi R_I^2}, \tag{3.12}$$

where a term $\gamma_1 \pi R_I^2$ is the area of two intersecting circles which comes from interference limit of primary receivers. Namely, according to the assumed interference model, there is a link in secondary network if both end nodes are at least R_I away from primary transmitters. In other terms, two circular regions centered corresponding two secondary nodes and with radii R_I must be free of primary users. Assuming the entire network has m channels, they derive the probability of at least one channel is available for two secondary nodes P_s as

$$P_s = 1 - (1 - P)^m = 1 - (e^{-\lambda_p \gamma_1 \pi R_I^2})^m. \tag{3.13}$$

Making use of multi-type branching process, clustering coefficient methods authors in [58] found necessary and sufficient conditions for full connectivity as follows

$$\lambda_s = \Theta\left(\frac{\log n}{r_s^2 \pi \mathbb{P}}\right). \tag{3.14}$$

and an upperbound on critical intensity of secondary users λ_s^c as follows

$$\lambda_s > \frac{1}{\pi r_s^2 \mathbb{P}(1 - \mathcal{C})}, \tag{3.15}$$

where $C = 1 - \frac{3\sqrt{3}}{4\pi}$ is a cluster coefficient defined in [59]. Authors in [47] used a percolation-based approach to study the connectivity of the two-tier network. PPP distributed primary network is parametrized with the density λ_p, communication range r_p, and the probability of primary link activity, while the connectivity of secondary network depends on density, communication r_s and interference tolerance r_i ranges of primary nodes. They prove that simultaneous percolation of both primary and secondary networks is impossible when the primary network operates in an *aggressive* mode, i.e. both probability of link activity and density is sufficient for percolation of the primary network (Figure 3.2). However, the last is related to only

instantaneous connectivity. For the scenario with primary link activity changing in time slotted manner, primary network with large enough density can still percolate in long term sense even if the probability of active link is not sufficient for instantaneous percolation (conservative region in Figure 3.2). Hence, allowing percolation of only secondary network at all time slots, [47] proved possibility of simultaneous *long term connectivity* of both networks. Moreover, it is important to note that [47] made the conclusion about non-feasibility of simultaneous instantaneous connectivity for only special case when $r_I > \max\{r_s, r_p\}^2$. One of the latest relevant works [48] proved that instantaneous percolation of two overlaying networks is actually possible, but if the following necessary conditions are hold:

$$\begin{aligned} &2r_{\mathrm{I}} > r_{\mathrm{s}}, \\ &\lambda_{\mathrm{s}} > r_{\mathrm{s}}^{-2}\lambda_{\mathrm{c}}(1), \\ &\lambda_{\mathrm{p}} > r_{\mathrm{p}}^{-2}\lambda_{\mathrm{c}}(1), \\ &\lambda_{\mathrm{p}} < \left(4r_{\mathrm{I}}^2 - r_{\mathrm{s}}^2\right)^{-1}\lambda_{\mathrm{c}}(1). \end{aligned} \tag{3.16}$$

[62] provide generic analysis for interferer-user type models such as cognitve network, jamming attack, shadowing effect. They consider conditions for percolation in a space of 3 parameters $(\lambda_s, \lambda_p, R_I)$, so called $3D$ connectivity region. They prove that $3D$ connectivity region is continuous in $(\lambda_s, \lambda_p, R_I)$ space and monotonic in the direction of axes. In particular, for fixed λ_s, a connectivity region surface curve is monotonically decreasing with R_I, while for fixed λ_p, it is monotonically increasing with λ_s. In addition, they derived sufficient and necessary conditions for percolation in terms of parameters $(\lambda_s, \lambda_p, R_I)$, which are as follows respectively

$$\left(1 - \exp\left(-\frac{\lambda_s r_s^2}{5}\right)\right)^2 \left(1 - \left(1 - e^{-\frac{\lambda_p}{N}\gamma\pi\left(R_p + \frac{r_s}{\sqrt{16}}\right)^2}\right)^N\right) > \frac{1}{2}, \tag{3.17}$$

$$r_p < \sqrt{\frac{N\lambda_c(1)}{\lambda_p} + \frac{r_p^2}{4}}, \tag{3.18}$$

where N is the number of channels.

[53] presents necessary and sufficient conditions for the k-connectivity of secondary user (SU) network in cognitive radio (CR). k-connectivity implies a type of connectivity where a network has an infinite size k-connected component. A component is said to be k-connected if, after removal of less than k vertices, a component still remains connected. An alternative definition for the k-connected component is when any two vertices in the component can be connected through k edge-disjoint paths. [32] derives closed-form expression for distribution of percolation degree. Percolation degree is the minimum number of neighbors for each node that will assure the k-connectivity of the network. So, we can notice that k-connectivity is similar to the k-nearest model, but the former one does not ignore the spatial communication range of nodes.

Y. Liu et al. . [33] studies the connectivity of secondary networks when connectivity within secondary users is defined with Random Connection Model. Specifically, at some time instance, t each link can be independently at either of two states 'reliable' or 'not reliable,' hence characterized by Bernoulli Random Variable X(t). Connectivity within secondary users f(d) is defined with the function $f(d) = Pr(X(t) = 1)$ which is assumed to be a non-increasing function of the distance between nodes d. As the work accounts for the time domain, three types of connectivity regimes are analyzed: disconnectivity, long term, and instantaneous connectivity (Fig.3.1). According to [33], the last two depend on the reliability of links, while disconnectivity does not.

Similar to Y. Liu et al. . [33], [44] incorporated the time into the scenario and worked with terms instantaneous and long term connectivity. However, for the latter, time variance is related to the spatial distribution of the primary network, but not

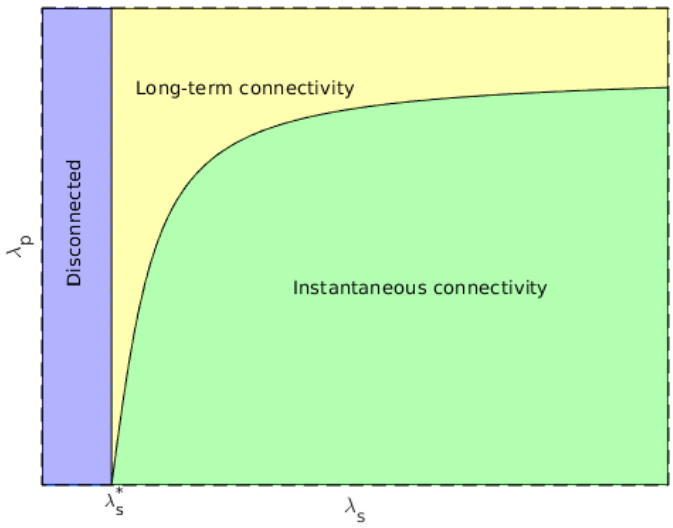

Figure 3.1: Connectivity region of secondary network in (λ_p, λ_s) plane

to the reliability of the links. W.Ren et al. in [44] assume temporal dynamics of the traffic in primary network keeping secondary one static. Specifically, PPP characterizing primary network is allowed to vary in each fixed time slot as the number of, and locations of active primary nodes may vary due to traffic change and motion of nodes. Meanwhile, PPP distributed secondary network is fixed. Connectivity of the network in the timely changing environment is characterized by finite delay (fd)-connectivity. The network is said to be fd-connected if the minimum multihop delay (MMD) between two random nodes of the network is finite with positive probability. [44] shows that with temporal dynamics of primary network density greater than the critical density of secondary users in a homogeneous network scenario (with no primary network) is sufficient condition for fd-connectivity regardless instantaneous densities of primary transmitters. Another difference of [44] from [33] is that the latter one assumes Gilbert disk model for connectivity, rather than RCM, hence considering only path loss and ignoring possible effects of shadowing and fading.

In [55], W. Ren et al., using continuum percolation, studied multi-hop delay in CRN and came to the following conclusions. In instantaneous connectivity region,

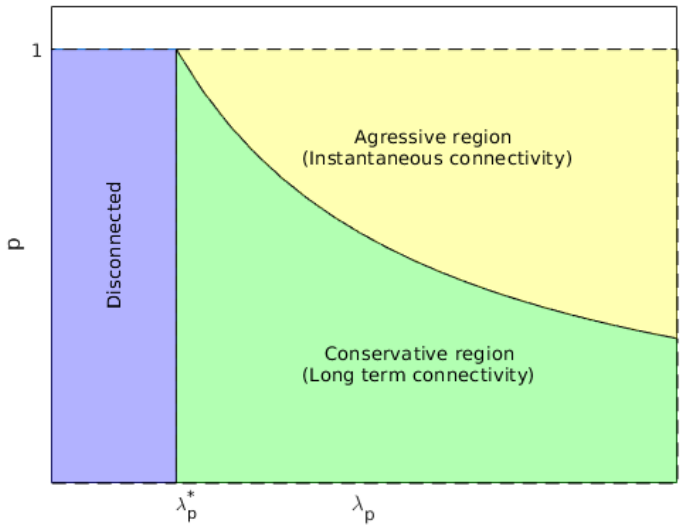

Figure 3.2: Connectivity region of secondary network in (p, λ_p) plane

the distance between two end nodes does not significantly affect to the asymptotic behavior of multihop delay while for long-term connectivity multihop delay is a linear function of the distance

In [34] for PPP distributed primary and secondary networks connectivity of secondary users is studied with consideration of probabilities of false alarm, correct and miss detection. They find an upper bound of critical intensity of secondary users for the network with fixed non-zero intensity of primary users $\lambda_s^c(\lambda_p)$, given critical intensity of secondary users for the network without primary users $\lambda_s^c(0)$

$$\lambda_s^c(\lambda_p) \geq \lambda_s^c(0) - \lambda_p \lambda_s^c(0) \eta \pi r_s^2 P_d - \lambda_s P_f \left(1 - \lambda_p \eta \pi r_s^2\right), \tag{3.19}$$

where P_d is the probability of detection and P_f is the probability of false alarm.

Another interesting case is presented in [43]. This work studies connectivity of secondary users with the account of internetwork interference and outage probability of primary users. For 2D space defined with transmit power and density of secondary users, Dong et al. found the upper and lower bounds of the percolation region. It

turned out that the percolation region is not always possible. In other words, an outage probability constraint of primary users and percolation of secondary users cannot always be both satisfied.

[45] accounts for probability of false alarm (P_f) and correct detection (P_d) in multi-channel cognitive radio network. The percolation problem is analyzed using the branching technique, namely degree distribution and generating function. [45] have verified that more number of channels may cause less tight bounds for percolation condition. In addition, it was shown that smaller Pf and larger Pd do not always improve the connectivity of SU.

Mapping continuum percolation model to discrete one, authors in [46] prove that in the space of (λ_s, λ_p) connectivity region of interference free cognitive radio network is a subset of connectivity region in interference-limited scenario. In other words, conditions allowing connectivity of SUs without interference also satisfy for the connectivity in the interference-limited network. The last leads to the conclusion that interference does not worsen the connectivity of SUs.

A study on connectivity in multi-channel CRN was conducted by [61]. Their model assumes fixed communication range based connectivity within networks and fixed protection range for primary users. A communication link in the graph is created if both geographical and radio links exist. A geographical link is created if two nodes satisfy a spatial proximity condition, while the radio link exists if both nodes have at least one common spectrum opportunity. The problem was analyzed using a newly introduced Cognitive Radio Graph Model (CRGM), where a multi-channel model was represented as a union of multi-layer graphs. They derived an upperbound on the critical density of primary nodes

$$\lambda_p^c < \frac{N \log(1 - \sqrt[N]{1 - \frac{\lambda_s}{\lambda_s}})}{2R_p^2 \left(\pi - \arccos \frac{r_s}{2R_s}\right) + r_s \sqrt{2R_p^2 - \frac{r_s^2}{4}}}. \tag{3.20}$$

A similar study on multi-channel access was conducted in [49]. According to their system model, connectivity within secondary nodes is defined based on 1)interference threshold and 2) common channel use between two end nodes of the link. It is assumed that each node of the network can choose a set of channels out of all available in a random manner. As two potentially connectable nodes share more than one common channel, the problem can be viewed as a multi-layered graph (MLG) (similar to CRGM). However, according to the second condition of connectivity, an edge between two nodes can be created if they share at least one common channel. So, it does not matter in what layer the connection is established, and we can simply take the union of all layers by mapping all existing edges from all layers to a single projection layer. Hence, the problem was solved using a 2-dimensional percolation model. Namely, for the described case, they show that even though interference and multiple channels worsen the connectivity in combination, these two are not always adverse.

A conclusion about the benefit of cooperation was also made by [54]. [54] study the scenario with the number of ad-hoc and infrastructure networks acting as secondary networks and coexisting with the number of primary interfering networks.

Ao et al. in [50,51] consider cognitive radio network with overlaying multiple PPP distributed secondary and primary networks. The system model accounts for interference at SU due to multiple primary networks, interference constraint at primary receivers due to SUs, and the effect of channel fading. For this kind of heterogeneous network, it was shown that cooperation improves connectivity. Cooperation here implies the case when a user of one secondary network relay through the user of another secondary network. Connectivity of typical secondary network was found by first deriving degree distribution of secondary users and the probability of active SUs. Those two findings are then applied in problem mapping to the site percolation model, which provides the percolation threshold.

[52] study Cognitive Radio-based operation of Device-to-Device ($D2D$) and cel-

lular network. The site percolation model is used to find an upper bound for the minimum probability of active transmission of devices that will assure large-scale connectivity of $D2D$ network in the presence of a primary cellular network.

[60] apply percolation to analyze probabilistic flooding in the interference-limited cognitive radio network. The objective was for each node to minimize the fraction of rebroadcasting neighbors P while keeping the network percolating. As the Boolean model is not appropriate for consideration of interference limit SINR percolation model discussed in [23] was used. Based on this analysis they propose novel Neighbor Aware Probabilistic Flooding (NAPF) method. The idea behind NAPF is to make the number of rebroadcasting neighbors always above percolation threshold, i.e more than $\lambda_s^c \pi R_s^2$, where λ_s^c critical intensity of SINR percolation model in CRN.

Applies percolation theory to study cooperation in CRN. Their system model assumes that a certain secondary user that falls within the interference range of primary transmitter can still be used as a relaying node in the way to achieve corresponding primary receiver. It is important to note that interference ranges are not fixed, but functions of outage probability thresholds of primary transmitters. Namely,

$$\lambda_P = \frac{\lambda_c(1)}{\left(r_f^D\right)^2 - \left(\frac{r_c^{sv}}{2}\right)^2}, \tag{3.21}$$

where r_f^D is radius of circular area around primary transmitter that approximate region where secondary networks can not be active except relaying secondary secondary node, and it is found as

$$r_f^D = \frac{r_I^{SR} + \max\left\{r_I^{SR}, r_I^{PR} + r_c^{PT}\right\}}{2}, \tag{3.22}$$

where

$$r_I^{SR} = \left[\frac{P_N}{P_{PT}}\left(\sqrt{1-\epsilon_{SR}}^{-\delta} - 1\right)\right]^{-\delta^{-1}}. \tag{3.23}$$

3.3 Percolation and Secrecy

Secrecy graphs were first introduced by M.Haengi in [74]. He gave geometry (distance) based definition for directed secrecy graphs (SGs).

Definition 7 (Directed SG. Distance-based definition [74])**.** Directed SG $\overrightarrow{G}_{sec}$ is a subgraph which includes all edges in the network satisfying

$$E = \left\{ \overrightarrow{x_i x_j} : |x_i - x_j| < |x_j - e_j^*| \right\}, \tag{3.24}$$

where e_j^* is the closest eavesroppper to x_j.

In other words, for $\overrightarrow{G}_{sec}$ a directed edge $\overrightarrow{x_i x_j}$ is created if x_i is closer to x_j than any other eavesdropper in the network. This work also introduced concepts of *basic* and *enhanced undirected SGs*.

Definition 8 (Strong undirected SG)**.** Undirected enhanced SG G_{sec}^{b} is a subgraph which includes all edges in the network satisfying

$$E = \left\{ \overline{x_i x_j} : |x_i - x_j| < \min(|x_j - e_j^*|, |x_i - e_i^*|) \right\}, \tag{3.25}$$

where e_i^* is the closest eavesdropper to x_i.

Definition 9 (Weak undirected SG)**.** Enhanced undirected SG G_{sec}^{e} is a subgraph which includes all edges in the network satisfying

$$E = \left\{ \overline{x_i x_j} : |x_i - x_j| < \max(|x_j - e_j^*|, |x_i - e_i^*|) \right\}, \tag{3.26}$$

Another contribution of this work is a derivation of a node out degree (Definition 4) distribution for directed SG . For the case, when legitimate users and eavesdroppers are independently PPP distributed with intensity 1 and λ respectively a node out

degree was found to be geometric with mean $\frac{1}{\lambda}$. For general case when intensity of legitimate users is λ a node out degrere is geometric with mean λ/λ_E, as given in [65]. Authors in [65] also derived moment generating function for a node in-degree, K_{in}

$$\mathbb{E}\left(e^{tK_{in}}\right) = \mathbb{E}\left(e^{A\left(e^{t}-1\right)/\lambda}\right), \tag{3.27}$$

where A is a cell area of Voronoi tessellation. As the tessellation is formed with PPP (of unit intensity) A is random variable. Hence, corresponding pmf of a node in-degree [14] is found as

$$\mathbb{P}(K_{in} = k) = \frac{1}{k!}\int_0^\infty f_2(t)e^{-t/\lambda}(t/\lambda)^k dt. \tag{3.28}$$

Unfortunately, $f_2(t)$, which is pdf of A, is still unknown. Moreover, a distribution of V_d, an equivalent of A in d-dimensional tesselation, remains an open question, except for $d = 1$.

Pinto et al. [12] gave the definition of secrecy graph from information-theoretic perspective. Namely, he made a connectivity function based on Maximum Secrecy Rate. Existence of phase transition for the given model was proven using 1) discrete percolation in hexagonal lattice, and 2) discrete percolation in square lattice and 3) a thinning property of PPP. As percolation does not guarantee connectivity of all nodes in the network, part of [12] was dedicated to full connectivity study.

Another important study of secrecy problems is given in [16]. Here, due to the unity AWGN assumption, a problem was reduced to distance-based secrecy graph, as in [74]. They studied both regular and random deployment of nodes. In the first case, legitimate users were placed at vertices of square/triangular lattice, while eavesdroppers appeared with some fixed probability inside a single square/triangle. If a square is intruded with at least one eavesdropper, all four legitimate users at vertices of that square will fail. The probability of having eavesdropper at a single

square/triangle was considered as percolation parameter. Lower and upper bounds for the critical probability of eavesdroppers in a square lattice denoted with p_c^E, were derived to be

$$1 - \frac{1}{\sqrt[16]{2}} \leq p_E^c \leq \frac{3-\sqrt{5}}{2}, \tag{3.29}$$

which was an improvement of previous result

$$\frac{1}{18} \leq p_E^c \leq \frac{3-\sqrt{5}}{2}, \tag{3.30}$$

obtained in [75].

Similarly, a critical probability for triangular lattice p_c^t, according to [16], is bounded as:

$$1 - \frac{1}{\sqrt[24]{2}} \leq p_c^t \leq \frac{4}{3} - \frac{1}{3}\left(\sqrt[3]{\frac{25-\sqrt{621}}{2}} + \sqrt[3]{\frac{25+\sqrt{621}}{2}}\right). \tag{3.31}$$

To model random deployment of legitimate nodes, they applied homogeneous PPP Φ of intensity 1. Their system model assumes that eavesdroppers' exact location is unknown. Instead, we know regions within which eavesdroppers may occur. Namely, they are circular regions with a fixed radius and centers distributed according to PPP Ψ, independent of Φ. Legitimate users are aware of those eavesdropper regions in which centers lie within the communication range of the users. So, another objective of the study was to explore the effect of uncertainty in the eavesdropper location. In particular, lower and upper bounds for mean node degree were derived analytically.

Another work with the random deployment of nodes in the secrecy graph is presented in [14]. The main difference of their system model from [16] is that eavesdroppers themselves, not centers of circles with eavesdroppers, are PPP distributed. In other words, in [14], there are no uncertainty regions associated with eavesdroppers. Another important remark, this work employs an original (distance-based [74]) defi-

nition of secrecy graphs. For the given case, [14] surveyed on techniques that can be used to find the critical intensity of eavesdroppers in directed SG. Namely, branching processes, mapping Gilbert disc model to lattice percolation, and rolling ball method were studied. Branching process could give an upper bound for critical eavesdropper intensity [1] $\lambda_E < 1$, while legitimate user intensity is 1. It was suggested that an infinite-dimensional geometric distribution branching process with a mean one could be a good approximation for the study of secrecy models in higher dimensions. According to [12, 65], a lattice, in particular, a hexagonal face, percolation can be used for secrecy graphs. Finally, the rolling ball method can give lower bound for the critical intensity of eavesdroppers in strong undirected secrecy graphs (Definition 9). Despite being a rigorous proof, all three methods gave loose bounds. Thus, [74] found more tighter bounds numerically with high confidence, based on [9, 76, 77].

R.Vaze and S.Iyer [11] enhanced Secrecy graphs by accounting for the effect of SINR and called it Information Secure SINR Graphs. Based on the analysis of super-critical and sub-critical percolation regimes [11] proved the existence of phase transition for Information Secure SINR Graphs. In addition, for fixed eavesdropper intensity, lower and upper bounds of the critical intensity of legitimate nodes were derived rigorously.

3.4 Conclusion

In this chapter, we reviewed wireless communication network works where percolation was applied. For convenience works were grouped under two large categories: connectivity and secrecy. Another possible application of percolation theory in a wireless network is security. Therefore, in the next chapter, we will explain how the percolation theory can be used to analyze the network epidemics problem.

[1] In the context of [14]), a critical intensity refers to infinite out-connected component

Chapter 4

Percolation Theory in Network Epidemics

4.1 Introduction

In this chapter, we will present the network epidemics problem in the context of the percolation theory. Namely, we will describe the system model as RGG and apply the concepts of percolation theory to find an efficient condition for the blockage of epidemics. Derived results will be verified with simulations.

4.2 System Model

As shown in Fig. 4.1, we consider a network that is composed of three types of nodes:
Susceptible nodes are regular nodes that have a potential to be infected with malware.
Anti-malware agents are nodes with special capability to cure all infected nodes within their coverage areas.
Protected nodes are regular nodes that fall within protection range of a anti-malware.
Throughout this thesis, both susceptible and protected nodes will be simply referred to as *regular nodes*.

Detailed definition of anti-malware agents anti-malware nodes are designed with special capability to filter detect infection in neighbour nodes(within fixed range) (e.g detect infection). In addition, anti-malware nodes are equipped with required

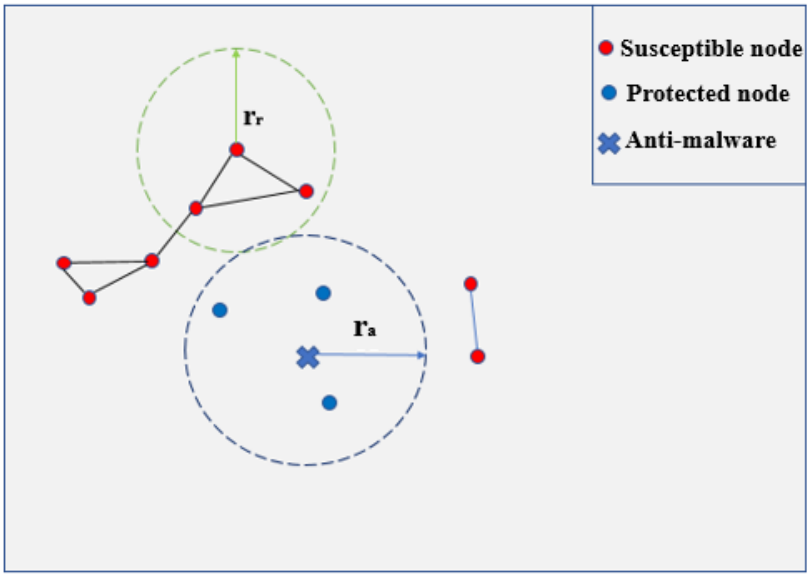

Figure 4.1: System model

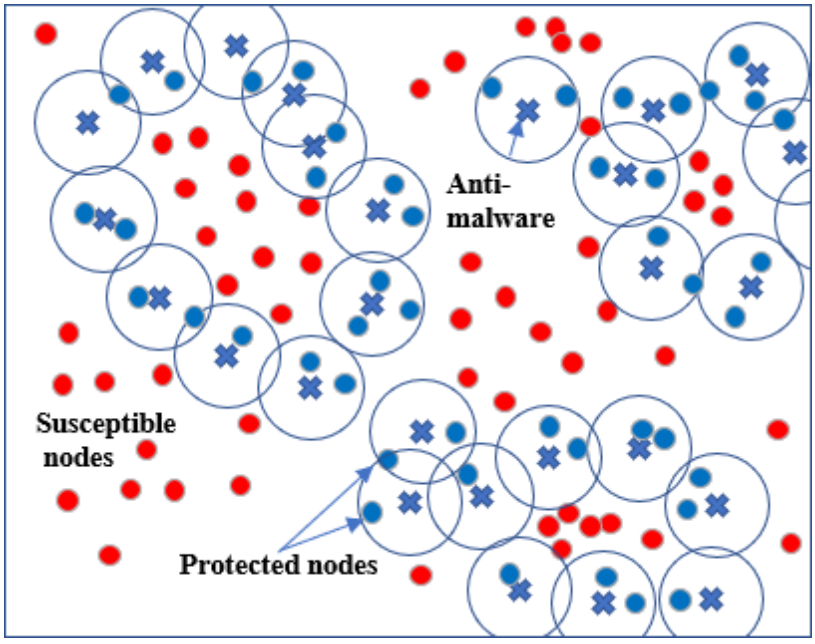

Figure 4.2: Epidemics blockage with antimalware

mechanisms and anti-malware software to implement on-demand software patching for the infected nodes within their range.

Assumptions

1. Distanced based connection: r_a and r_r are communication range of anti-malware and regular nodes,respectively.
2. $r_a \geq r_r$
3. Malware type: Worm
4. Topology: ad-hoc wireless network
5. All regular nodes have no other seciruty system other than antimalware

Let us comment on some of the above assumptions. The second assumption is introduced to fit the analysis constraints, discussed later in this chapter. However, even from a practical perspective, this assumption seems to be meaningful. Nodes with special capabilities, such as anti-malware, tend to have greater coverage range compared to regular communication nodes.

With regards to the third assumption, viruses and Trojans cause harm to the system if an infected file is exchanged or/and executed while worm spread happens automatically without host interventions. Therefore, Worm spreads more easily and hence represents the highest security threat, compared to Virus and Trojan. So, to consider the worst-case scenario, we assume Worm as a specific malware type of our system model.

According to the last assumption, all nodes, except protected by anti-malware nodes, are vulnerable to infection via communication link. In practise, it is not always the case because usually all devices are empowered with built-in firewalls which are supposed to protect from malware intrusions. Malware passes from one node to another

if there is faults in the protection system of the destination. So, existence of communication link does not guarantee infection spread. However, condition for blockage of epidemics in the scenario when all nodes are vulnerable to infection by simply creating communication link will also work when not all nodes are susceptible to infection. So, with assumption 5, we will deal with the worst-case scenario and hence, get simplified analysis with generally valid results.

The regular nodes (devices) are scattered in $\mathbb{R}^2$, where their locations are modeled as a Poisson Point Process (PPP) $\Phi \equiv \{x_i\} \in \mathbb{R}^2$ with intensity λ_r. These devices can communicate if they are within distance r_r from each other. In addition, we model the locations of anti-malware agentsas a PPP $\Psi \equiv \{a_k\} \in \mathbb{R}^2$ with intensity λ_a, independent of Φ, and have a fixed detection range r_a. The network of regular users is modeled as Random geometric graph G(V, E), where V, standing for a set of vertices, includes $\forall x_k \in \Phi_r$, and E refers to the set of edges, which reflects susceptible links between regular nodes. Hence, E can be formally defined as follows

$$E = \{\overline{x_i x_j} : |x_i - x_j| \leq r_r \wedge |x - a| \geq r_a\}, \tag{4.1}$$

where $x = x_i, x_j$, $a = arg \min_{a_k \in \Psi} |x - a_k|$, r_a and r_r are communication range of anti-malware agents and regular nodes respectively. The above definition implies that malware can transfer from one regular node to another only if both of them are not within the protection zone of anti-malware nodes.

4.3 Problem formulation

Recalling (4.1), we observe that the percolation of G(V, E) implies the susceptibility of the network to malware. In particular, due to percolation, the infection of one node might lead to an epidemic throughout the network. Hence, the objective is to employ enough anti-malware agents to ensure breaking the giant component into

smaller, isolated components, as shown in Fig. 4.2. This, in turn, ensures a contained outbreak that can be quarantined and recovered.

4.4 Phase transition

The first main result in this thesis is proving the existence of critical value for the density of anti-malware agents λ_a^c. A formal description of this result is provided next.

Theorem 3 (Phase transition)**.** *Let $\theta(\lambda_a)$ denote the percolation probability of G(V,E), then for $\forall \lambda_r > 0$ there exists a critical value $\lambda_a^c < \infty$ for the density of curing agents such that*

$$\begin{aligned} \theta(\lambda_a) &> 0, \quad \textit{for } \lambda_a < \lambda_a^c \\ \theta(\lambda_a) &= 0, \quad \textit{for } \lambda_a > \lambda_a^c \end{aligned} . \tag{4.2}$$

Proof. As mentioned in Chapter. 4 discrete percolation model is simpler for analysis. Hence, the proof of phase transition will include the following steps

1. Mapping our problem to discrete percolation model in hexagonal lattice, we prove that $\forall \lambda_r > 0$ there exists some $\lambda_L < \infty$ such that $\theta(\lambda_a) > 0$, for $\lambda_a < \lambda_L$. Hence, we will study *subrcritical* regime.

2. Mapping our problem to discrete percolation model in square lattice we prove that $\forall \lambda_r > 0$ there exists some $\lambda_U < \infty$ such that $\theta(\lambda_a) = 0$, for $\lambda_a > \lambda_U$. Hence, we will study *supercritical* regime.

3. Finally, using basic properties of PPP we prove that $\theta(\lambda_a)$ is a continuous non-increasing function of λ_a, hence show that there should be some critical λ_a^c reflecting phase transition of the system. [12].

4.4.1 Subcritical regime:

In this part we will assume that $r_r = r_a$. As it will be discussed later the condition that assures percolation in $r_r = r_a$ also works for the case when $r_r \leq r_a$.

Proposition 4 (Sufficient condition for zero percolation)**.** *For* $\forall \lambda_r > 0$ *and* $r_r > 0$ *if*

$$\lambda_a > \frac{3.65}{r_r^2}, \tag{4.3}$$

then $\theta(\lambda_a) = 0$.

Proof. **Mapping to a Hexagonal Lattice:** Let $\mathcal{L}_h$ be hexagonal lattice with side equal to communication range of regular nodes r_r. In discrete model each hexagon $\mathcal{H}$ composing L_h is called a face which can be of either *open* or *closed* state.

Definition 10 (Closed face)**.** Let $\{T_i\}_{i=1}^3$ denote non-adjacent equilateral triangles composing $\mathcal{H}$ as shown in fig.. Then, a face $\mathcal{H}$ is said to be closed if each of these triangles is occupied with at least one anti-malware agent.

Otherwise, it is called *open face*. Definition 10 was chosen, such that no percolation in $\mathcal{L}_h$ assures no percolation in the given continuum model. Sequence of connected closed faces form *a closed path*. If a path starts and ends at the same face, then it is called a *closed circuit*, Fig. 4.4. Referring back to our scenario closed face can be analogically treated as anti-malware in the discrete model and set of open faces surrounded by the closed circuit as a confined region of infection.

Lemma 5 (Circuit coupling)**.** *Let* $K^G(0) \subseteq G(V, E)$ *and* $K^h(0) \subseteq \mathcal{L}_h$ *denote a connected component around the origin* [1] *in the given continuum and discrete models respectively. If the origin is surrounded with closed circuit* $\mathcal{C}(0)$ *in* $\mathcal{L}_h$ *then* $K^G(0)$ *is finite*

[1] Due to homogeneity of PPP without loss of generality we can assume that the infection starts at the origin

Proof. If there is a closed circuit around the origin, there are a finite number of open faces on the inner side of the circuit. Hence, $|K^h(0)| < \infty$ [2]. and a region covered by $K^h(0)$ involves finite number vertices of $G(V, E)$. So, if we prove that no edge of G(V, E) cross $C(0)$, then we prove that $K^G(0)$ is finite. So, let us consider an extreme scenario shown in Fig. 4.3. Assume each of the triangles T has only one anti-malware (the lowest possible according to Definition 10), and they are placed in a way to get the minimum coverage of the closed face. By minimizing coverage of anti-malware agents, we can see how close two regular nodes (red dots) from different sides of $C(0)$ can get to each other without being neutralized by agents. So, now let us consider the critical position of regular nodes shown in Fig.4.3. Since the lattice side equals r_r, two red nodes can communicate, but they fall within the coverage region of anti-malware agents. If nodes move apart, they will no longer be affected by anti-malware agents, but now they are out of the communication range of each other. If they move closer communication range is satisfied, but they will appear under the protection region of anti-malware agents. So, both conditions of edge existence can never be satisfied simultaneously, and hence, no edge can cross $\mathcal{C}$. If we find the conditions for no percolation when $r_r = r_a$, the result will also work for the case when $r_a \geq r_r$ as the probability of percolation decreases with an increase of r_a. Since the lattice side equals to the communication range of nodes, two regular nodes can establish the connection. However, according to Definition 10 x_i and x_j appear under guard zone of at least one agent, even if the agent is at the furthest possible position, which is corresponding vertices of the hexagon (See Fig.4.3). So, we can conclude that a link crossing $C(0)$ does not exist even in most favorable conditions for communication, and according to the previous reasoning $|K^h(0)| < \infty$.

□

Lemma 6 (Closed circuit in $\mathcal{L}_h$)**.** *if* $\forall \lambda_r > 0$ *and* $r_r > 0$*, the following condition is*

[2] $|.|$ denotes a cardinality of the component

satisfied

$$\left(1 - e^{-\lambda_a \frac{\sqrt{3}}{4} r_r^2}\right)^3 > \frac{1}{2}, \tag{4.4}$$

then $\mathcal{C}(0)$ *exists in* $\mathcal{L}_h$.

Proof. According to [78] the origin is a.s surrounded with closed circuit C(0) in $\mathcal{L}_h$ if

$$P(\mathcal{H} \text{ is closed}) > \frac{1}{2}. \tag{4.5}$$

Probability of closed face, according to Definition 10, is

$$\begin{aligned} &P(\mathcal{H} \text{ is closed }) = \mathrm{P}\left(\wedge_{i=1,2,3} |T_i \cap \Phi| \geq 1\right) \\ &\overset{(a)}{=} \left(1 - \mathrm{P}\left(|T_1 \cap \Phi_f| = 0\right)\right)^3 = \left(1 - e^{-\lambda_a} \frac{\sqrt{3}}{4} r_r^2\right)^3, \end{aligned} \tag{4.6}$$

where (a) is due to the fact that $\{T_i\}_{i=1}^3$ are identical and non-overlapping regions.

Substituting (4.6) into (4.5) we get the condition stated in Lemma 6.

□

Rearranging the terms of (4.4) and following to the statement of Lemma 5 we can reach that there is a closed circuit $\mathcal{C}(0)$ in $\mathcal{L}_h$ if $\lambda_a > 3.65/r^2$. Meanwhile according to Lemma 6 existence of $\mathcal{C}(0)$ assures $K^h(0) < \infty$. So, $\lambda_a > 3.65/r^2$ is the condition that guarantees $G(V, E)$ does not percolate which finalize the proof of Proposition 4. □

4.4.2 Super-critical regime:

Proposition 7 (Sufficient condition for positive percolation probability)**.** *If* $r_r > 0$ λ_a *satisfies*

$$\lambda_a < \frac{2\ln\left(1 - e^{-\lambda_r s^2}\right) - \ln\left(1 - \beta\right)}{N_A s^2}, \tag{4.7}$$

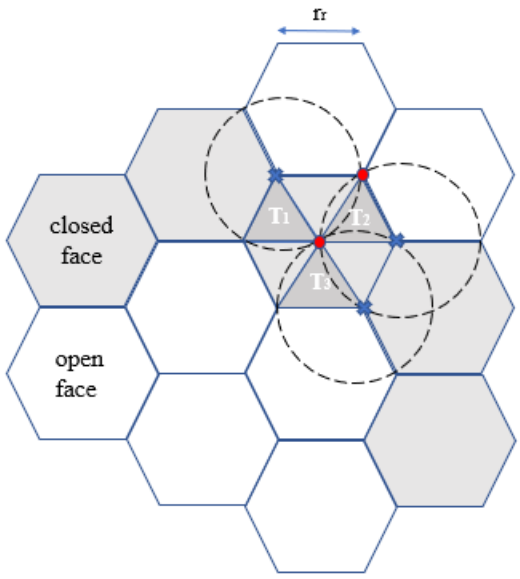

Figure 4.3: Closed face

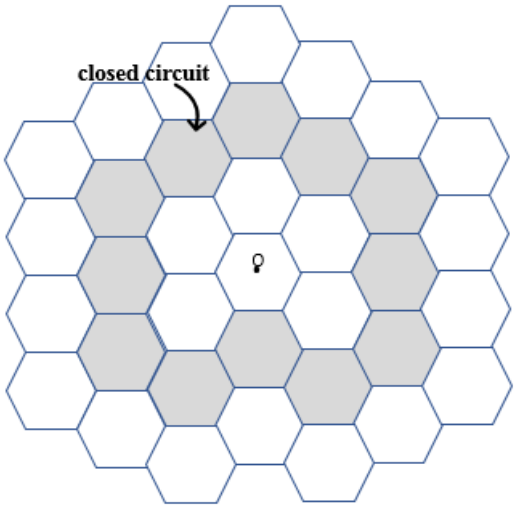

Figure 4.4: Closed circuit

where $\beta = (\frac{11-2\sqrt{10}}{27})^N$, N *and* N_A *are some finite integers,* $s = \frac{r_r}{\sqrt{5}}$, *then* $\theta(\lambda_a) > 0$.

Proof. **Mapping to a Square Lattice:** Let $\mathcal{L}_s$ be a square lattice with side $s = r_r/\sqrt{5}$. A dual lattice $\mathcal{L}_s^d$ is defined by the following transition $\mathcal{L}_s + (\frac{s}{2}; \frac{s}{2})$ and we assume one of vertices of $\mathcal{L}_s^d$ is the origin of coordinate system. Let e denote an edge common to two adjacent squares $S_1(e)$ and $S_2(e)$ in $\mathcal{L}$ and e^d is the corresponding dual edge in $\mathcal{L}_s^d$. and e can be either *open* or *closed*.

Definition 11 (Open edge)**.** Let $\{ v_k\}_{k=1}^4$ denote vertices of a rectangle compounded by $S_1(e)$ and $S_2(e)$ and $A(e)$ is the smallest square containing circles $\{C(v_k, r_a)\}_{k=1}^4$. Then an edge e is defined to be open iff:

1. both $S_1(e)$ and $S_2(e)$ have at least one regular node
2. there are no anti-malware agents within $A(e)$.

As the diagonal of $S_1(e) \cup S_2(e)$ equals to r_r any two regular nodes within this rectangle are at a distance allowing to establish communication. Moreover, condition 2 in Definition 11 requires that all anti-malware lie outside region $A(e)$. So, even if regular node lies at the boundaries of $S_1(e) \cup S_2(e)$ any anti-malware will be at a distance $\lceil \frac{\sqrt{5}r_a}{r_r} \rceil \frac{r_r}{\sqrt{5}} + \epsilon_1 > r_a$, where $\epsilon_1 > 0$. Hence, no regular node inside $S_1(e) \cup S_2(e)$ can be neutralized. So, if e is open according to (4.1) any two nodes within $S_1(e) \cup S_2(e)$ satisfy for conditions of edge existence. Hence, all nodes within this region create one connected component. In general, Definition 11 was chosen such that percolation in L_s^d assures percolation in $G(V, E)$ as we will see later.

Lemma 8 (Dual and primal coupling)**.** *Let $\mathcal{K}^s(0)$ denote connected component containing origin in L_s^d. If $\mathcal{K}^s(0)$ is infinite then $\mathcal{K}^G(0)$ is also infinite.*

Proof. Let a path $\mathcal{P}^d$ denote a sequence of connected open edges in $\mathcal{L}_s^d$. Since there is one to one mapping between dual and prime edges $\mathcal{P}^d$ is uniquely associated with another path $\mathcal{P}$ in $\mathcal{L}_s$ which all edges are also open. In its turn, $\mathcal{P}$ is associated with sequence of $(S1(e_i), S2(e_i))$ pairs where each pair composed of single connected component of regular nodes according to the Definition 11. So, if infinite path is given in L_s^d then there is infinite sequence of connected components which merge and create one infinite connected component in G(V,E). In other words, if $\mathcal{K}^s(0) < \infty$ then $\mathcal{K}^G(0) < \infty$. □

So, to study supercritical regime in $G(V, E)$ it is sufficient to investigate percolation condition in L_s^d.

Percolation in $\mathcal{L}_s^d$: From the relation between dual and primal square lattices we can notice that $K^d(0)$ is finite if there is closed path in $\mathcal{L}_s$. So, first, we will study the probability of path $P_n := \{e_i\}_{i=1}^n$ in $\mathcal{L}_s^d$ being closed around 0. Let $B(e)$ be the smallest square containing circles $\left\{C(e_i, \sqrt{5}s + 2r)\right\}_{i=1}^4$ [3]. The region $B(e)$ was defined such that edges e_i and e_j are independent if $(B(v_i) \cap B(v_j)) = \emptyset$.

Let $C(e)$ be the region which covers all edges dependent from edge e and N denote the number of edges in $C(e)$. Let $S^I \subset P_n$ denote a subset which includes all independent edges in P_n. Then the S^I will have cardinality at https://www.overleaf.com/project/5e5e89d005 n/N. The way to construct C(e) and compute N is given in Appendix 5.

According to [1] a circuit of length n around the origin can be created in $4n3^{n-2}$ different ways. Therefore, a probability that a closed path exists about the origin P_c can be found as

$$\begin{aligned} P_c = \sum_{n=1}^{\infty} 4n3^{n-2} P(\mathcal{P}_n \text{ is closed}) &\leq \sum_{n=1}^{\infty} 4n3^{n-2} p^{\frac{n}{N}} \\ &\overset{\text{(b)}}{=} \frac{4p^{\frac{1}{N}}}{3(1-3p^{\frac{1}{N}})^2}, \end{aligned} \tag{4.8}$$

where $p := P(e \text{ is closed})$ and (b) is obtained by treating a given sum as a derivative of geometric series with respect to $p^{1/N}$. So, to make P_c to not exceed 1, the following must be satisfied

$$p < (\frac{11 - 2\sqrt{10}}{27})^N. \tag{4.9}$$

Based on the Definition 11 explicit expression for p can be found as follows

$$\begin{aligned} p = 1 - P(|\Phi \cap S_1(e)| \geq 1 \wedge \\ |\Phi \cap S_2(e)| \geq 1 \wedge |A(e) \cap \Psi| = 0) \\ = 1 - (1 - e^{-\lambda_r s^2})^2 e^{-\lambda_a N_A s^2}, \end{aligned} \tag{4.10}$$

[3] $C(\mathcal{O}, R)$ is the circle with radius R and center at $\mathcal{O}$

where N_A is the number of squares covered by $A(e)$, hence. From fig. 4.5 $N_a = (2\lceil\frac{\sqrt{5}r_a}{r_r}\rceil + 2) \times (2\lceil\frac{\sqrt{5}r_a}{r_r}\rceil + 1)$.

Substituting (4.10) into (4.9) and after basic algebraic manipulation we can finally get the result in (4.7). □

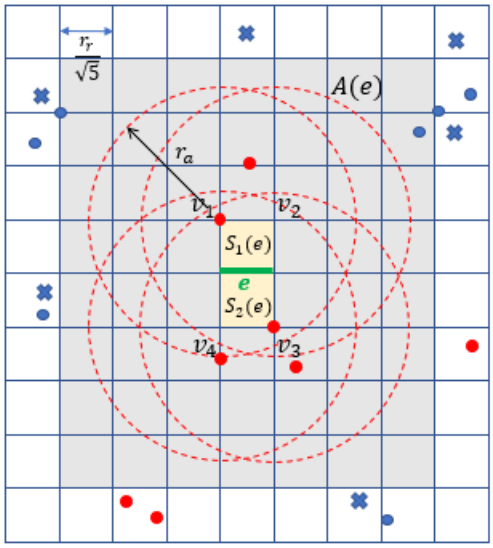

Figure 4.5: Closed face

From Proposition 4 we can conclude that for some given $\lambda_r > 0$ and $r_r > 0$ there exists a threshold $\lambda_L < \infty$ such that the probability of percolation $\theta(\lambda_a) > 0$, $\forall\lambda_a < \lambda_L$. On the other hand, according to Proposition 7 there is a threshold λ_U such that $\theta(\lambda_a) = 0\ \forall\lambda < \theta_2$. Thus, to verify that there exists $\lambda_L \leq \lambda_a^c \leq \lambda_U$ such that Theorem 3 is true we need to show that $\theta(\lambda_a)$ is a continuous non-increasing function of λ_a.

4.4.3 Continuity of Percolation probability

Proposition 9. *For fixed λ_r, r_r, r_a $\theta(\lambda_a)$ is a continuous non-increasing function of λ_a.*

Proof. Consider random geometric graphs $G(\lambda_{a_1})$ and $G(\lambda_{a_2})$ where $0 < \lambda_{a_1} < \lambda_{a_2}$ and parameters λ_r,r_r and r_a are the same for both processes. As underlying processes

of $G(\cdot)$ is PPP $G(\lambda_{a_1})$ can be obtained by thinning $G(\lambda_{a_2})$ with probability $\frac{\lambda_{a_1}}{\lambda_{a_2}}$. As thinning implies random removal of nodes $G(\lambda_{a_1})$ should have less number of anti-malware agents compared to $G(\lambda_{a_2})$. Correspondingly, more susceptible nodes are supposed to stay non-neutralized in the first case compared to the second one. So, it is valid to state that $K^{G(\lambda_{a_1})}(0) \geq K^{G(\lambda_{a_2})}$. As a consequence, the following is true

$$\theta(\lambda_{a_1}) \geq \theta(\lambda_{a_2}),$$

for $0 < \lambda_{a_1} < \lambda_{a_2}$ which literally implies that $\theta\lambda_a$ is non-increasing function of λ_a. □

□

Despite being useful for the proof of phase transition, bounds in (4.3) and (4.7) are not tight enough and of no practical value. So, in the following section, we will compute a tight upper bound for the critical value of the density of curing agents λ_a^c.

4.5 An upper bound for λ_a^c

Theorem 10. *An upper bound for the critical density of anti-malware agents is*

$$\lambda_f^c \leq \frac{\lambda_c(1)}{4r_a^2 - r_r^2}, \tag{4.11}$$

where $\lambda_c(1)$ is a critical density of nodes for continuum percolation in Gilbert disk model with radius 1/2. Based on simulations [79], $\lambda_c(1) \approx 1.44$. We also know that $0.768 < \lambda_c(1) < 3.37$ [80, 81]. To keep the analysis rigorous, we will use the upper bound for $\lambda_c(1)$.

Proof. Proof of Theorem 3 relies on the fact that the existence of an infinite connected component in the network of regular nodes implies the existence of an infinite vacant component in the network of anti-malware agents. Let us consider the worst-case arrangement shown in Fig. 4.6. Two regular nodes are placed at a distance of r_r, and

they will remain to be susceptible if all anti-malware agents are forced to be at least r_a away from them. So, the position of anti-malware in Fig.4.6 is of special interest. In this arrangement region, V depicts the vacant space that must be provided by the network of anti-malware agents such that two regular nodes are able to communicate, and r_O is the minimum distance from the anti-malware agent to V. Therefore, the minimum requirement for the existence of an infinite path in the network of regular nodes is having an infinite vacant component in the Poisson Boolean model with density λ_a and radius $r_o := \sqrt{r_a^2 - \frac{r_r^2}{4}} - \frac{\epsilon_2}{2}$. Critical density for homogeneous Boolean model with radius r [28] is

$$\frac{\lambda_c(1)}{(2r)^2}.$$

So, there is an infinite vacant component a.s. in the network of anti-malware agents if

$$\lambda_a^c < \frac{\lambda_c(1)}{(2\sqrt{r_a^2 - \frac{r_r^2}{4}} - \epsilon_2)^2}.$$

Leting $\epsilon_2 \longrightarrow 0$ we will finally get the uppperbound in (4.11). □

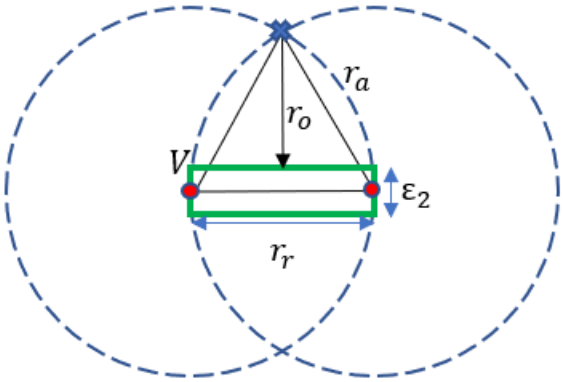

Figure 4.6: Worst case scenario for existence of infinite path

4.6 Results and Discussion

In this section, we will first verify the existence of phase transition for the model described in Sec. 4. Then, we validate the upperbound for critical density of anti-malware agents is rigorously derived in Sec.4.

4.6.1 Methodology

The described network scenario was implemented in Matlab. Two types of points were scattered over the finite square region of size 100×100. We set parameters r_a and r_r much smaller than 100 and λ_r and λ_a sufficiently small so that connectivity over this finite region reasonably approximates large scale percolation. Percolation is assumed to happen if there is a connected component crossing the simulation region from left to right (or vice versa) or from bottom to top (or vice versa). Percolation probability is estimated with Monte Carlo simulations with 200 realizations.

4.7 Simulation results

For the network parameters $r_a = r_r = 2$, $\lambda_r = 0.8$ we verified a phase transitional behavior described in Theorem 3 (See Fig.4.7). Following the definition of critical density, λ_a^c appears at the point when percolation probability drops to 0 for the first time. Therefore, we can notice that with the increase of r_r λ_a^c gets smaller. Next, for the same network setup by tuning λ_r corresponding critical density of anti-malware agents were obtained. Region falling below and above the blue curve in Fig. 4.8 depict connectivity (percolation) and disconnectivity (no percolation) conditions respectively. So, from Fig.4.8 we can conclude that the upper bound, computed according to (4.11) and shown with orange line in Fig.4.8, is tight and assures no percolation of regular users $\forall \lambda_r$.

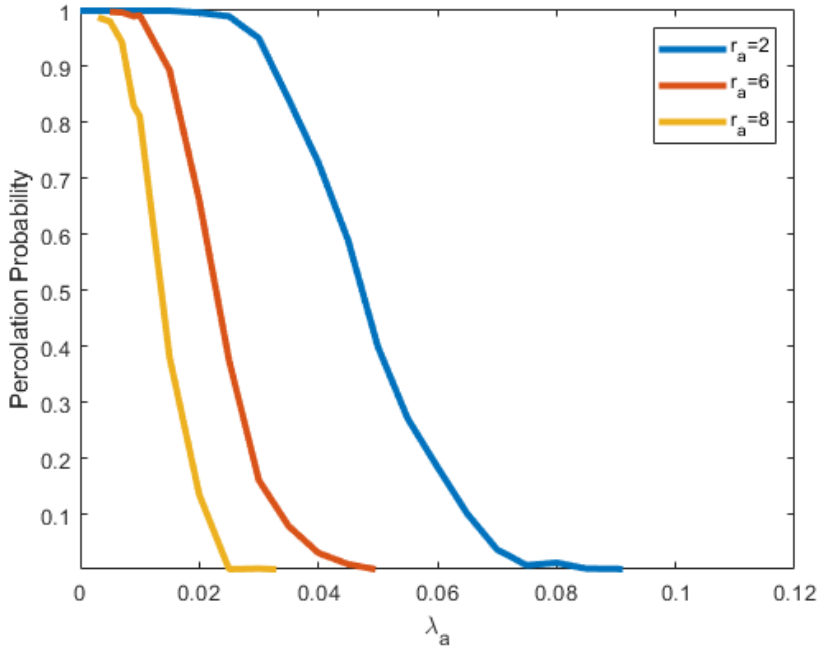

Figure 4.7: Phase transition

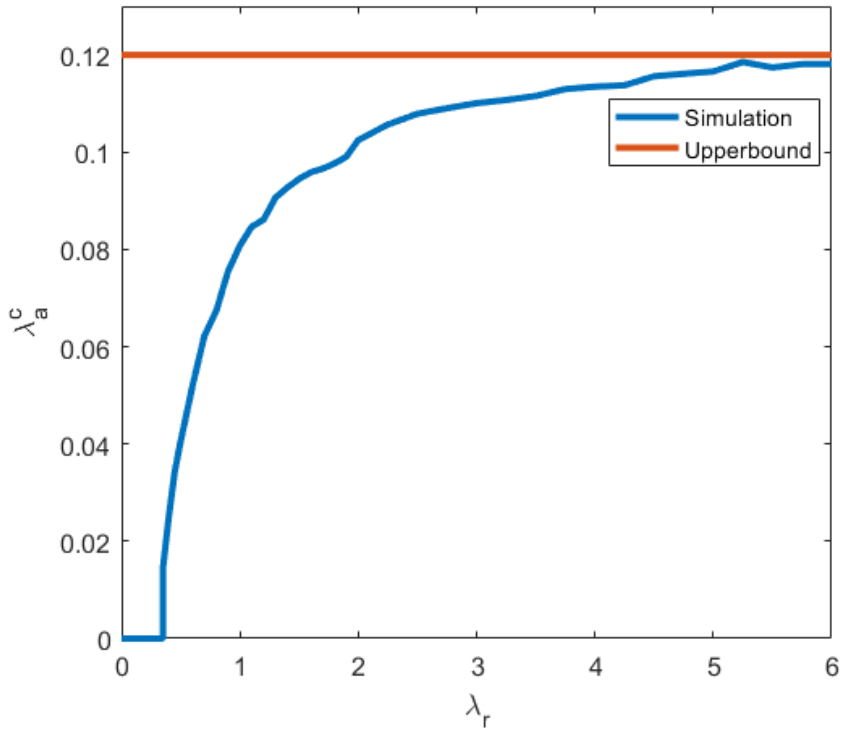

Figure 4.8: Upperbound for critical intensity of anti-malware agents

4.8 Conclusion

In this chapter, we discussed the results obtained with Matlab Simulations. Namely, the effect of the communication range of anti-malware agents on the phase transition threshold was investigated. The anti-malware density condition for the blockage of large scale epidemics was verified.

Chapter 5

Conclusion and Future work

Motivated by the evolving size of IoT and, hence, the need for cybersecurity over long distances, this thesis arose the topic of large scale network epidemics. We proposed the solution for the problem based on the spatial deployment of firewalls. The idea was to make the number of added firewalls sufficient to have epidemics confined over the finite region and, at the same time, reasonable considering the finiteness of resources. To meet both these requirements, a powerful math tool, percolation theory, was employed. To sum up, this thesis includes two major contributions. First, we made a detailed survey on the topic of percolation theory in wireless communication networks. Secondly, we provided a solution for network epidemics problems and related analyses based on the percolation theory. We have proved the existence of critical value for the density of curing agents above which malware outbreaks are prevented. Furthermore, a tight upper bound for the critical density was computed and validated.

A possible extension of the work is to make planned spatial deployment of anti-malware agents. By planned deployment, we imply placing anti-malware agents such that a larger number of regular nodes are under coverage region of anti-malware. For example, we can try to set anti-malware near the node with a maximum number of neighbors. This arrangement should increase the chance that anti-malware will appear at locations with the largest accumulation of regular nodes.

APPENDICES

A.1 Maximum number of dependent edges

Here, we will try to find the maximum number of edges that are dependent of some arbitrary edge e_0. Let us assume that all edges in the lattice have dependency region X(e) of general size $a \times b$ squares. According to the definition of dependency region two edges e_i, e_j are considered independent iff $(X(e_i) \cap X(e_j)) = \emptyset$. Therefore, let $\{e_n\}_{n=1}^{8}$ be 8 the closest edges which dependency regions $\{X(e_i)\}_{i=1}^{8}$ do not overlap with $X(e)$. Next, we should construct maximal rectangle around e_0 such that created region X_0 does not include $\{e_i\}_{i=1}^{8}$ (example shown in fig.A.1). Hence, we can be sure that X_0 covers maximal number of edges that are dependent of e_0. By construction the size of X_0 is $(2a-2) \times (2b-1)$. So, the number of edges in X_0, correspondingly the maximum number of edges dependent from e_0, is $[(2a-1)(2b-1)+(2a-2)2b] = 8ab-2a-6b+1$.

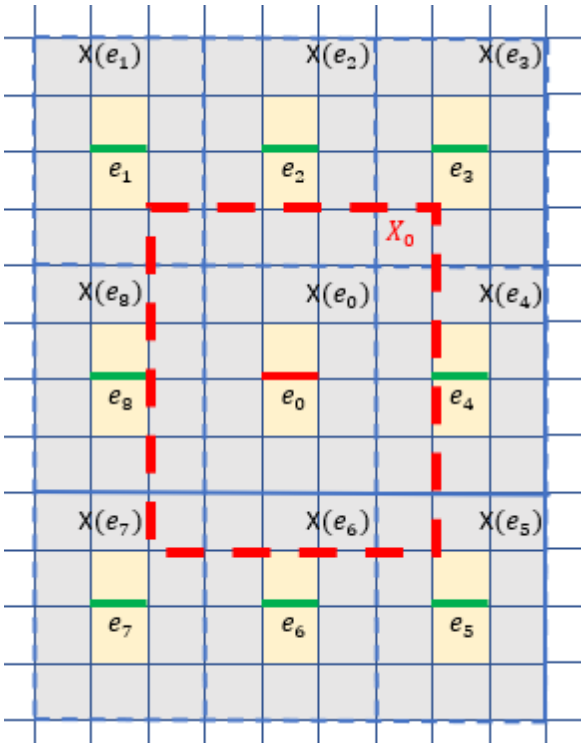

Figure A.1: An edge dependence region

REFERENCES

[1] G.Grimmett, *Percolation*. Springer-Verlag, 1980.

[2] M. Haenggi, *Stochastic Geometry for Wireless Networks*. Cam-bridge Univ. Press, 2012.

[3] M. E. Fisher and J. W. Essam, "Some cluster size and percolation problems," *Journal of Mathematical Physics*, vol. 2, pp. 609–619, 1961.

[4] Y. Z. Xiangyun Zhou, Lingyang Song, *Physical Layer Security in Wireless Communications*. CRC Press, 2013.

[5] M. F. Sykes and J. W. Essam, "Exact critical percolation probabilities for site and bond problems in two dimensions," *Journal of Mathematical Physics*, vol. 5, p. 1117â1127, 1964.

[6] M. Hori and K. Kitahara, "Percolation thresholds for honeycomb,kagome and triangular lattices," in *International Conf. StatisticalPhysics*, 2004.

[7] O. HÃ¤ggstrÃ¶m and R. Meester, "Nearest neighbor and hard sphere models in continuum percolation," *Random Structures Algorithms*, vol. 9, no. 3, pp. 295–315, 10 1996. [Online]. Available: https://doi.org/10.1002/(SICI)1098-2418(199610)9:3⟨295::AID-RSA3⟩3.0.CO;2-S

[8] S.-H. Teng and F. F. Yao, "k-nearest-neighbor clustering and percolation theory," *Algorithmica*, vol. 49, no. 3, pp. 192–211, Nov 2007. [Online]. Available: https://doi.org/10.1007/s00453-007-9040-7

[9] P. N. Balister and B. Bollobás, "Percolation in the k-nearest neighbor graph," 2008.

[10] F. Xue and P. Kumar, "The number of neighbors needed for connectivity of wireless networks," *Wireless Networks*, vol. 10, no. 2, pp. 169–181, Mar 2004. [Online]. Available: https://doi.org/10.1023/B:WINE.0000013081.09837.c0

[11] R. Vaze and S. Iyer, "Percolation on the information theoretic secure sinr graph: Upper and lower bounds," in *10th International Workshop on Spatial Stochastic Models for Wireless Networks 2014*, Hammamet, Tunisia, 2014.

[12] P. C. Pinto and M. Z. Win, "Percolation and connectivity in the intrinsically secure communications graph," *IEEE Transactions on Information Theory*, vol. 58, no. 3, pp. 1716 – 1730, Mar. 2012.

[13] P. Pinto, J. Barros, and M. Z. Win, "Wireless secrecy in large-scale networks," in *2011 Information Theory and Applications Workshop*, La Jolla, CA, USA, 2011.

[14] A.Sarkar and M. Haenggi, "Percolation in the secrecy graph," in *2011 Information Theory and Applications Workshop*, La Jolla, CA, USA, 2011.

[15] A.Sarkar and M.Haenggi, "Percolation in the secrecy graph: Bounds on the critical probability and impact of power constraints," in *2011 Information Theory Workshop*, Paraty, Brazil, 2011.

[16] S. Goel, V. Aggarwal, A. Yener, and A. R. Calderbank, "The effect of eavesdroppers on networkconnectivity: A secrecy graph approach," *IEEE TRANSACTIONS ON INFORMATION FORENSICS AND SECURITY*, vol. 6, p. 712â724, 2011.

[17] X. Jia, J.-S. Hong, C. Yang, C.-J. Fu, and J.-Q. Hu, "A two-stage percolation process in random networks," in *2015 Asia-Pacific Microwave Conference (APMC)*, Nanjing, China, 2015.

[18] W. Fan, D. Gaogao, D. Ruijin, and T. Lixin, "Robustness of multiple interdependent networks under shell attack," in *2017 36th Chinese Control Conference (CCC)*, Dalian, China, 2017.

[19] Q. Zhang, D. Li, R. Kang, E. Zio, and P. Zhang, "Reliability analysis of interdependent networks using percolation theory," in *2013 International Conference on Signal-Image Technology Internet-Based Systems*, Kyoto, Japan, 2013.

[20] O. Dousse, F. Baccelli, and P. Thiran, "Impact of interferences on connectivity in ad hoc networks," *IEEE/ACM Transactions on Networking*, vol. 13, pp. 425 – 436, Apr. 2005.

[21] M. F. Olivier Dousse, N. Macris, and P. Thiran, "Percolation in the signal to interference ratio graph," *Journal of Applied Probability*, pp. 552 – 562, 2006.

[22] O. Al-Tameemi and M. Chatterjee, "Percolation in multi-channel secondary cognitive radionetworks under the sinr model," in *2014 IEEE International Symposium on Dynamic Spectrum Access Networks*, McLean, VA, USA, 2014.

[23] O. Al-Tameemi, M. Chatterjee, and A. Al-Rumaithi, "Percolation condition for interference-limited cognitive radio networks," in *2014 IEEE 25th Annual International Symposium on Personal, Indoor, and Mobile Radio Communication*, Washington, DC, USA, 2014.

[24] O. Al-Tameemi, M. Chatterjee, K. Kwiat, and C. Kamhoua, "Napf: Percolation driven probabilistic flooding for interference limited cognitive radio networks," in *2015 IEEE International Conference on Communications (ICC)*, London, UK, 2015.

[25] B. BÅaszczyszyn and D. Yogeshwaran, "Connectivity in sub-poisson networks," in *2010 48th Annual Allerton Conference on Communication, Control, and Computing (Allerton)*, Allerton, IL, USA, 2010.

[26] M. Yemini, A. Somekh-Baruch, R. Cohen, and A. Leshem, "On Simultaneous Percolation with Two Disk Types," *arXiv e-prints*, p. arXiv:1601.04471, Jan 2016.

[27] A.Sarkar and M.Haenggi, "Continuum percolation with holes," *Statistics Probability Letters*, vol. 126, pp. 212–218, 2017.

[28] W.Ren, Q.Zhao, and A.Swami, "Connectivity of heterogeneous wireless networks," *IEEE Transactions on Information Theory*, vol. 56, pp. 4315–4332, 2011.

[29] L. Liu, X. Zhang, and H. Ma, "Optimal density estimation for exposure-path prevention in wireless sensor networks using percolation theory," in *2012 Proceedings IEEE INFOCOM*, Orlando, FL, USA, 2012.

[30] X. Gu and H. Feng, "Connectivity analysis for a wireless sensor network based on percolation theory," in *2012 Proceedings IEEE INFOCOM*, Orlando, FL, USA, 2012.

[31] Y. Katada, "Physical-layer security in stochastic wireless networks," in *2014 IEEE/SICE International Symposium on System Integration*, Tokyo, Japan, 2014.

[32] L. Fu, L. Qian, X. Tian, H. Tang, N. Liu, G. Zhang, and X. Wang, "Percolation degree of secondary users in cognitive networks," *IEEE Journal on Selected Areas in Communications*, vol. 30, no. 10, pp. 1994–2005, November 2012.

[33] Y. Liu, Y. Cui, and X. Wang, "Connectivity and transmission delay in large-scale cognitive radio ad hoc networks with unreliable secondary links," *IEEE Transactions on Wireless Communications*, vol. 14, no. 12, pp. 7016–7029, Dec 2015.

[34] D. Liu, E. Liu, Z. Zhang, R. Wang, Y. Ren, Y. Liu, I. W. Ho, X. Yin, and F. Liu, "Secondary network connectivity of ad hoc cognitive radio networks," *IEEE Communications Letters*, vol. 18, no. 12, pp. 2177–2180, Dec 2014.

[35] L. Liu, X. Zhang, and H. Ma, "Optimal density estimation for exposure-path prevention in wireless sensor networks using percolation theory," in *2012 Proceedings IEEE INFOCOM*, March 2012, pp. 2601–2605.

[36] J. Wang and X. Zhang, "3d percolation theory-based exposure-path prevention for optimal power-coverage tradeoff in clustered wireless camera sensor networks," in *2014 IEEE Global Communications Conference*, Dec 2014, pp. 305–310.

[37] H. M. Ammari and S. K. Das, "Critical density for coverage and connectivity in three-dimensional wireless sensor networks using continuum percolation," *IEEE Transactions on Parallel and Distributed Systems*, vol. 20, no. 6, pp. 872–885, June 2009.

[38] L. Liu, X. Zhang, and H. Ma, "Bond-percolation based optimal density for exposure-path prevention in wireless sensor networks," in *IEEE GLOBECOM 2008 - 2008 IEEE Global Telecommunications Conference*, Nov 2008, pp. 1–5.

[39] Xin Gu and Hailin Feng, "Connectivity analysis for a wireless sensor network based on percolation theory," in *2010 International Conference on Computer Application and System Modeling (ICCASM 2010)*, vol. 5, Oct 2010, pp. V5–203–V5–207.

[40] D. Penkin, G. Janssen, and A. Yarovoy, "Source node location estimation in large-scale wireless sensor networks," in *2012 42nd European Microwave Conference*, Oct 2012, pp. 333–336.

[41] G. Franceschetti, S. Marano, and F. Palmieri, "Percolation model for urban area propagation: results and open problems," in *IEEE Antennas and Propagation Society International Symposium (IEEE Cat. No.02CH37313)*, vol. 1, June 2002, pp. 224–227 vol.1.

[42] Y. Katada, "Connectivity of swarm robot networks for communication range and the number of robots based on percolation theory," in *2014 IEEE/SICE International Symposium on System Integration*, Dec 2014, pp. 93–98.

[43] D. Liu, E. Liu, Y. Ren, Z. Zhang, R. Wang, and F. Liu, "Bounds on secondary user connectivity in cognitive radio networks," *IEEE Communications Letters*, vol. 19, no. 4, pp. 617–620, April 2015.

[44] W. Ren, Q. Zhao, and A. Swami, "Temporal traffic dynamics improve the connectivity of ad hoc cognitive radio networks," *IEEE/ACM Transactions on Networking*, vol. 22, no. 1, pp. 124–136, Feb 2014.

[45] D. Liu, E. Liu, Y. Ren, Z. Zhang, D. Wang, R. Wang, P. Wang, F. Liu, and C. H. Liu, "Node density and connectivity of multi-channel ad hoc cognitive radio

networks," in *2015 IEEE/CIC International Conference on Communications in China (ICCC)*, Nov 2015, pp. 1–6.

[46] Y. Guo, Y. Ma, K. Niu, and J. Lin, "Connectivity of interference limited cognitive radio networks," in *2012 3rd IEEE International Conference on Network Infrastructure and Digital Content*, Sep. 2012, pp. 158–163.

[47] Q. Zhou, L. Gao, and S. Cui, "Connectivity of two-tier networks," in *2010 IEEE Globecom Workshops*, Dec 2010, pp. 368–372.

[48] M. Yemini, A. Somekh-Baruch, R. Cohen, and A. Leshem, "The simultaneous connectivity of cognitive networks," *IEEE Transactions on Information Theory*, vol. 65, no. 11, pp. 6911–6930, Nov 2019.

[49] O. A. Al-Tameemi and M. Chatterjee, "Percolation in multi-channel secondary cognitive radio networks under the sinr model," in *2014 IEEE International Symposium on Dynamic Spectrum Access Networks (DYSPAN)*, April 2014, pp. 170–181.

[50] W. C. Ao, S. Cheng, and K. Chen, "Connectivity of multiple cooperative cognitive radio ad hoc networks," *IEEE Journal on Selected Areas in Communications*, vol. 30, no. 2, pp. 263–270, February 2012.

[51] W. C. Ao and K. Chen, "Percolation-based connectivity of multiple cooperative cognitive radio ad hoc networks," in *2011 IEEE Global Telecommunications Conference - GLOBECOM 2011*, Dec 2011, pp. 1–6.

[52] M. G. Khoshkholgh, Y. Zhang, K. Chen, K. G. Shin, and S. Gjessing, "Connectivity of cognitive device-to-device communications underlying cellular networks," *IEEE Journal on Selected Areas in Communications*, vol. 33, no. 1, pp. 81–99, Jan 2015.

[53] L. Fu, Z. Liu, D. Nie, and X. Wang, "K-connectivity of cognitive radio networks," in *2012 IEEE International Conference on Communications (ICC)*, June 2012, pp. 83–87.

[54] W. C. Ao and K. Chen, "Cognitive radio-enabled network-based cooperation: From a connectivity perspective," *IEEE Journal on Selected Areas in Communications*, vol. 30, no. 10, pp. 1969–1982, November 2012.

[55] W. Ren, Q. Zhao, and A. Swami, "On the connectivity and multihop delay of ad hoc cognitive radio networks," *IEEE Journal on Selected Areas in Communications*, vol. 29, no. 4, pp. 805–818, April 2011.

[56] ——, "Connectivity of heterogeneous wireless networks," *IEEE Transactions on Information Theory*, vol. 57, no. 7, pp. 4315–4332, July 2011.

[57] ——, "On the connectivity and multihop delay of ad hoc cognitive radio networks," in *2010 IEEE International Conference on Communications*, May 2010, pp. 1–6.

[58] L. Sun and W. Wang, "On the connectivity of large multi-channel cognitive radio networks," in *2012 IEEE International Conference on Communications (ICC)*, June 2012, pp. 1854–1858.

[59] Z. Kong and E. M. Yeh, "Analytical lower bounds on the critical density in continuum percolation," in *2007 5th International Symposium on Modeling and Optimization in Mobile, Ad Hoc and Wireless Networks and Workshops*, April 2007, pp. 1–6.

[60] O. A. Al Tameemi, M. Chatterjee, K. Kwiat, and C. Kamhoua, "Napf: Percolation driven probabilistic flooding for interference limited cognitive radio networks," in *2015 IEEE International Conference on Communications (ICC)*, June 2015, pp. 7534–7539.

[61] D. Lu, X. Huang, P. Li, and J. Fan, "Connectivity of large-scale cognitive radio ad hoc networks," in *2012 Proceedings IEEE INFOCOM*, March 2012, pp. 1260–1268.

[62] Y. Liu, C. Li, C. Yin, and H. Dai, "A unified framework for wireless connectivity study subject to general interference attack," in *2015 IEEE International Conference on Communications (ICC)*, June 2015, pp. 7174–7179.

[63] O. Dousse, F. Baccelli, and P. Thiran, "Impact of interferences on connectivity in ad hoc networks," *Proceedings - IEEE INFOCOM*, vol. 3, pp. 1724–1733, 9 2003.

[64] O. Dousse, F. Baccelli, and P. Thiran, "Impact of interferences on connectivity in ad hoc networks," *IEEE/ACM Transactions on Networking*, vol. 13, no. 2, pp. 425–436, April 2005.

[65] P. C. Pinto, J. Barros, and M. Z. Win, "Physical-layer security in stochastic wireless networks," in *2008 11th IEEE Singapore International Conference on Communication Systems*, Guangzhou, China, 2008.

[66] P. Balister, B. BollobÃ¡s, A. Sarkar, and M. Walters, "Connectivity of random k-nearest-neighbor graphs," *Mathematics*, vol. 37, no. 1, pp. 1–24, 2005.

[67] Z. Kong and E. M. Yeh, "Directed percolation in wireless networks with interference and noise," *CoRR*, vol. abs/0712.2469, 2007. [Online]. Available: http://arxiv.org/abs/0712.2469

[68] O. Dousse, M. Franceschetti, N. Macris, R. Meester, and P. Thiran, "Percolation in the signal to interference ratio graph," *Journal of Applied Probability*, vol. 43, no. 2, p. 552â562, 2006.

[69] D. J. Daley, "The definition of a multi-dimensional generalization of shot noise," *Journal of Applied Probability*, vol. 8, no. 1, p. 128â135, 1971.

[70] R. Vaze, "Percolation and connectivity on the signal to interference ratio graph," in *2012 Proceedings IEEE INFOCOM*, March 2012, pp. 513–521.

[71] B. Jahnel and A. Tóbiás, "Sinr percolation for cox point processes with random powers," 2019.

[72] M. Franceschetti, O. Dousse, D. N. C. Tse, and P. Thiran, "Closing the gap in the capacity of wireless networks via percolation theory," *IEEE Transactions on Information Theory*, vol. 53, no. 3, pp. 1009–1018, March 2007.

[73] X. Li, Y. Liu, S. Li, and S. Tang, "Multicast capacity of wireless ad hoc networks under gaussian channel model," *IEEE/ACM Transactions on Networking*, vol. 18, no. 4, pp. 1145–1157, Aug 2010.

[74] M. Haenggi, "The secrecy graph and some of its properties," in *2008 IEEE International Symposium on Information Theory*, Toronto, ON, Canada, 2008.

[75] S. Goel, V. Aggarwal, A. Yener, and A. R. Calderbank, "Modeling location uncertainty for eavesdroppers: A secrecy graph approach," in *2010 IEEE International Symposium on Information Theory*, Austin, TX, USA, 2010.

[76] B. BollabÃ¡s and A. Stacey, "Approximate upper bounds for the critical probability of oriented percolation in two dimensions based on rapidly mixing markov chains," *Journal of Applied Probability*, vol. 34, no. 4, p. 859â867, 1997.

[77] P. Balister, B. BollobÃ¡s, and M. Walters, "Continuum percolation with steps in the square or the disc," *Random Structures & Algorithms*, vol. 26, no. 4, pp. 392–403, 2005. [Online]. Available: https://onlinelibrary.wiley.com/doi/abs/10.1002/rsa.20064

[78] B. BollobÃ¡s and O. Riordan, *Percolation*. Cambridge University Press, 2006.

[79] J. Quintanilla, S. Torquato, and R. M. Ziff, "Efficient measurement of the percolation threshold for fully penetrable discs," *Journal of Physics A: Mathematical and General*, vol. 33, no. 42, pp. L399–L407, oct 2000.

[80] R. Meester and R. Roy, *Continuum Percolation*. New York: Cambridge Univ. Press, 1996.

[81] Z. Kong and E. M. Yeh, "Characterization of the critical density for percolation in random geometric graphs," in *2007 IEEE International Symposium on Information Theory*, June 2007, pp. 151–155.